JOC The Journal of Organic Chemistry

Article

pubs.acs.org/joc

Switchable Protecting Strategy for Solid Phase Synthesis of DNA and RNA Interacting Nucleopeptides

Maria Emilia Mercurio,[†,⊥] Stefano Tomassi,[†,⊥] Maria Gaglione,[†] Rosita Russo,[†] Angela Chambery,[†] Stefania Lama,[§] Paola Stiuso,[§] Sandro Cosconati,[†] Ettore Novellino,[‡] Salvatore Di Maro,*[,†] and Anna Messere*[,†]

[†]Department of Environmental, Biological and Pharmaceutical Sciences and Technologies, Second University of Naples, Via Vivaldi 43, 81100 Caserta, Italy

[‡]Department of Pharmacy, University of Naples "Federico II", Via D. Montesano 49, 80131 Napoli, Italy

[§]Department of Biochemistry, Biophysics and General Pathology, Second University of Naples, Via De Crecchio 7, 80127 Napoli, Italy

Supporting Information

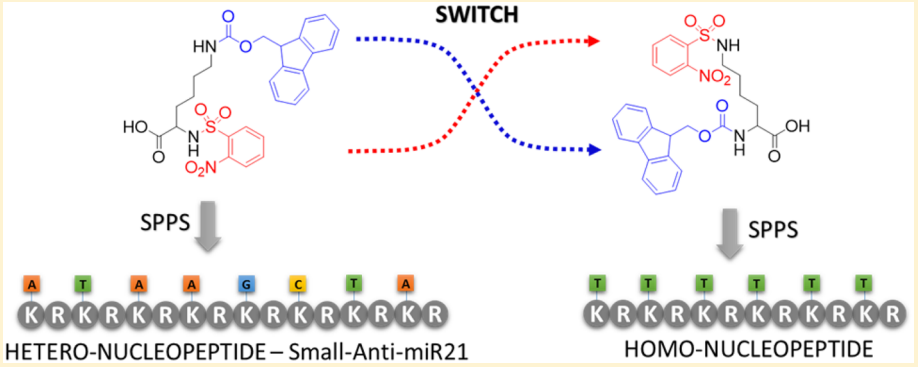

ABSTRACT: Nucleopeptides are promising nucleic acid mimetics in which the peptide backbone bears nucleobases. They can recognize DNA and RNA targets modulating their biological functions. To date, the lack of an effective strategy for the synthesis of nucleopeptides prevents their evaluation for biological and biomedical applications. Herein, we describe an unprecedented approach that enables the synthesis of cationic both homo and heterosequence nucleopeptides wholly on solid support with high yield and purity. Spectroscopic studies indicate advantageous properties of the nucleopeptides in terms of binding, thermodynamic stability and sequence specific recognition. Biostability assay and laser scanning confocal microscopy analyses reveal that the nucleopeptides feature acceptable serum stability and ability to cross the cell membrane.

INTRODUCTION

MicroRNAs[1] (miRNAs), recently uncovered effectors for RNA interference (RNAi) gene regulation mechanism, result dysregulated in several human diseases, representing an attractive target for therapeutic applications.[2,3] Inhibition of overexpressed miRNAs may be achieved by 20−23 in length anti-miRNA oligonucleotides (AMOs). Unfortunately, their application is often hampered by limited biostability, low binding affinity, poor cellular delivery, and nonspecific stimulation of the immune system.[4] Recently, a more attractive strategy based on the targeting of the sole miRNA "seed region"[5] by octanucleotide congeners,[6−8] enabled to partially address the aforementioned limitations. In this respect, peptide nucleic acids (PNAs) represent the most promising DNA mimics (Figure 1).[9] PNAs bind the single-stranded DNA and RNA with high affinity and specificity following the Watson−Crick base pairing rules and form very stable duplexes even in low ionic strength solutions. These properties, together with the high biostability

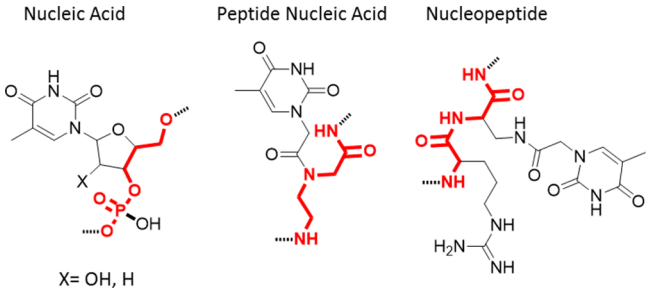

Figure 1. Nucleic acid, PNA, and nucleopeptide backbone units comparison.

of PNAs allowed for broad applications, such as inhibition of target microRNA function both *in vitro* and *in vivo*.[10,11] On the

Received: July 28, 2016
Published: October 28, 2016

DOI: 10.1021/acs.joc.6b01829
J. Org. Chem. 2016, 81, 11612−11625

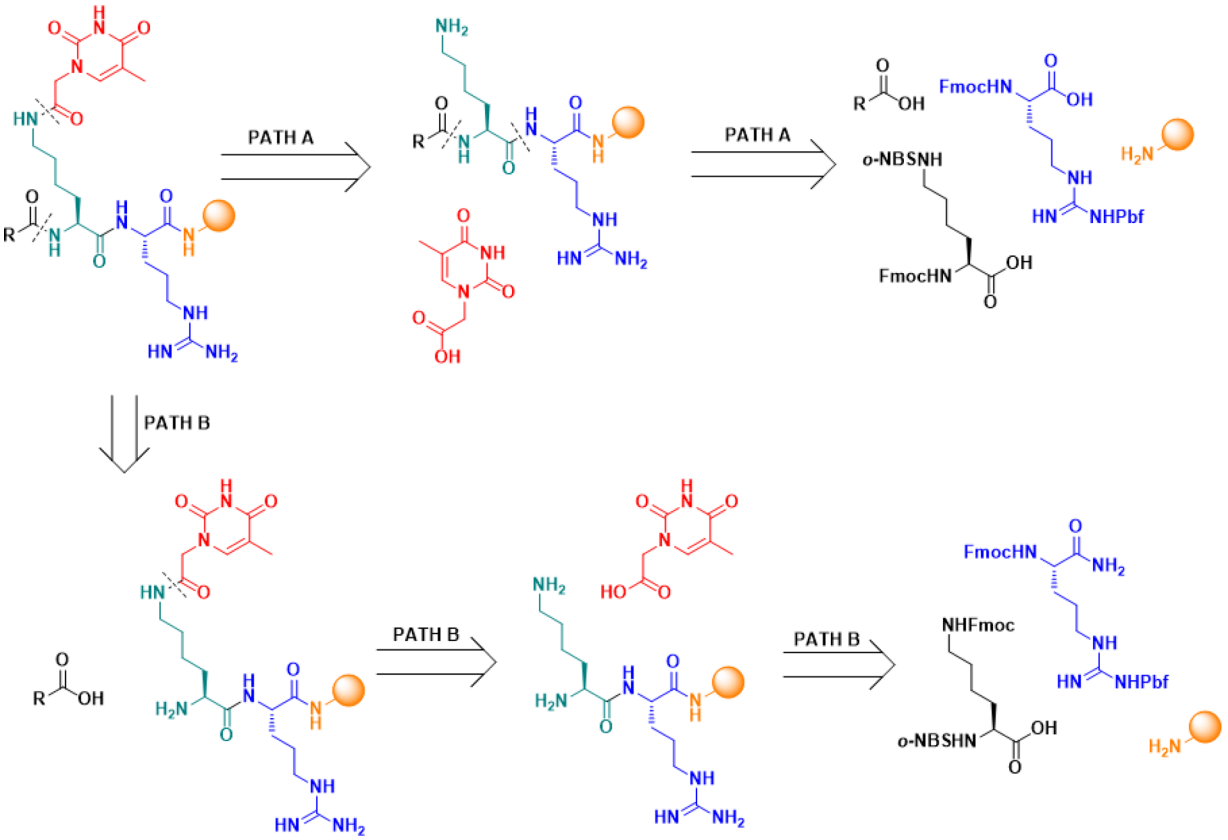

Figure 2. Retrosynthetic analysis of homo- (PATH A) and heteronucleopeptide monomers (PATH B).

other hand, problems still exist in the use of PNAs as real therapeutics, mainly due to their poor cell membrane permeability, low aqueous solubility, and sequence dependent self-aggregation. In an effort to overcome these limitations, several strategies were explored, including PNA conjugation,[12,13] formulation,[14,15] and chemical modifications of the PNA backbone.[16−18] As part of the ongoing studies aiming to develop alternative structures to PNAs, a new class of molecules known as nucleopeptides gained considerable biological relevance.[19−21] Nucleopeptides combine both the polyarginine cell penetrating peptide (CPP)[22] features critical for cell uptake, and the specificity of recognition of nucleic acids (Figure 1). They differ from conventional conjugates because the delivery and recognition elements are integrated into a single component. Indeed, nucleopeptides hybridizing DNA and RNA are polymers in which the repeating unit is made up by a nucleobase-substituted amino acid and an underivatized residue. A previous study reported the binding properties toward poly deoxy-adenylic acid (polydA) and poly adenylic acid (polyA) of a thymine-functionalized nucleopeptide, composed of alternating thymine-bearing L-Lys and underivatized L-Arg residues.[23]

Unfortunately, the tremendous potential of this new class of molecules has not been fully disclosed yet, mainly because of the lack of a versatile synthetic strategy that can assist for the synthesis of both homo- and heteronucleobase sequences. While so far the described strategy allowed only the synthesis of thymine homosequences, we can anticipate that obtaining heterosequences is not an easy task considering the need to prepare in solution the four fully protected nucleo-amino acids.

In this study, we aimed at bridging this gap by describing the development of a facile and powerful synthetic method that enables, for the first time, the synthesis of both homo- and hetero- cationic nucleopeptides wholly on solid support with a high yield and a high degree of purity. Here, the DNA and RNA binding properties of synthesized nucleopeptides were also investigated by CD, UV spectroscopic techniques, and compared with the corresponding DNA and RNA sequences. A further characterization of the RNA hybrid complex was carried out by RP-HPLC and ESI Q-TOF MS spectrometry. Finally, cellular uptake and human serum biostability properties were investigated using laser scanning confocal microscopy and HPLC and MALDI/TOF MS analyses, respectively.

RESULTS AND DISCUSSIONS

Rationale Design and Building Blocks Synthesis. With aim to obtain new molecules able to bind specific nucleic acid targets and to cross the cellular barriers, we designed nucleopeptides alternating cell-penetrating components (cationic residues) and recognition elements (nucleobases). In DNA and RNA isomorphous nucleopeptides, two amino acids span the length of six bonds in the sugar−phosphate backbone (Figure 1).[24] Thus, a dipeptide residue bearing a nucleobase represents the monomeric unit mimicking a single nucleotide. In our nucleopeptides, the monomer was designed selecting L-Lys and L-Arg residues. In particular, L-Lys was employed to introduce the suitable derivatized nucleobase, while L-Arg was chosen due to the large number of studies indicating this amino acid as main component of the CPP. Moreover, to validate our synthetic approach, we preferred L-amino acids for the backbone building because of cost and availability-related reasons.

The preparation of nucleopeptides relies on two orthogonal protecting groups at α and ε positions of L-Lys residues that can be easily switched based on the need to synthesize homo- or heterosequences (Figure 2). As first protecting group, we

DOI: 10.1021/acs.joc.6b01829
J. Org. Chem. 2016, 81, 11612−11625

Scheme 1. Synthesis of the Nucleopeptide Building Blocks

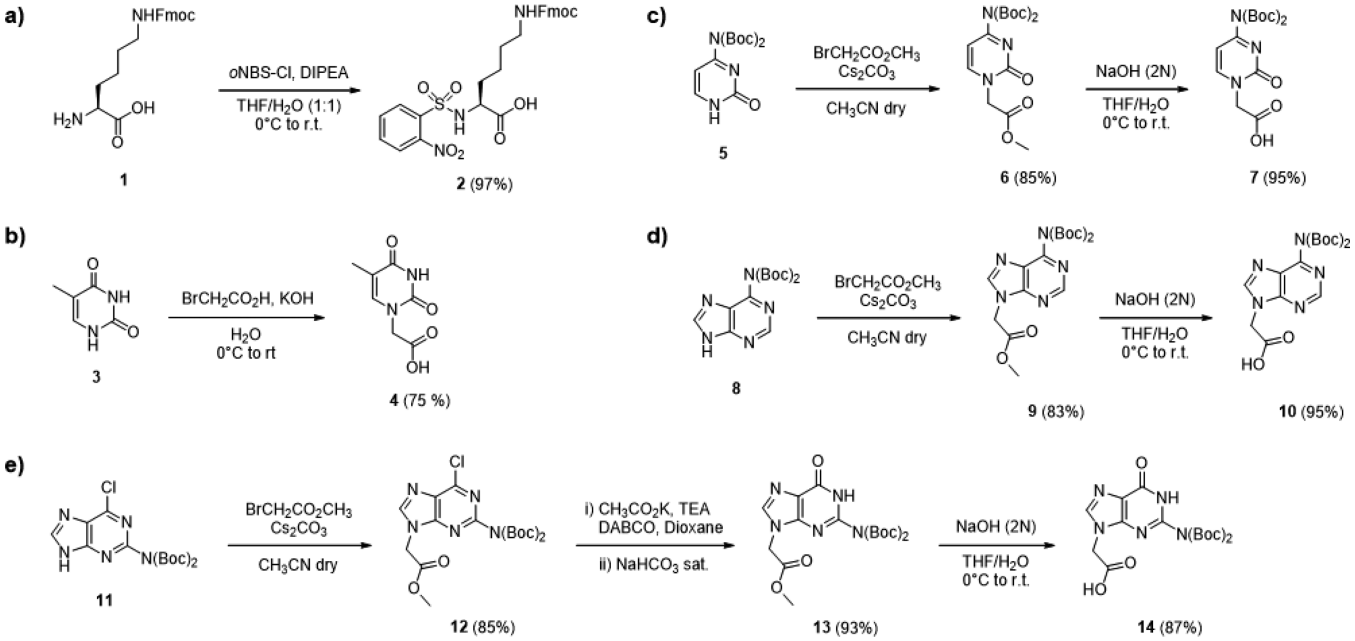

Scheme 2. Synthetic Route to Homonucleopeptides 21-23

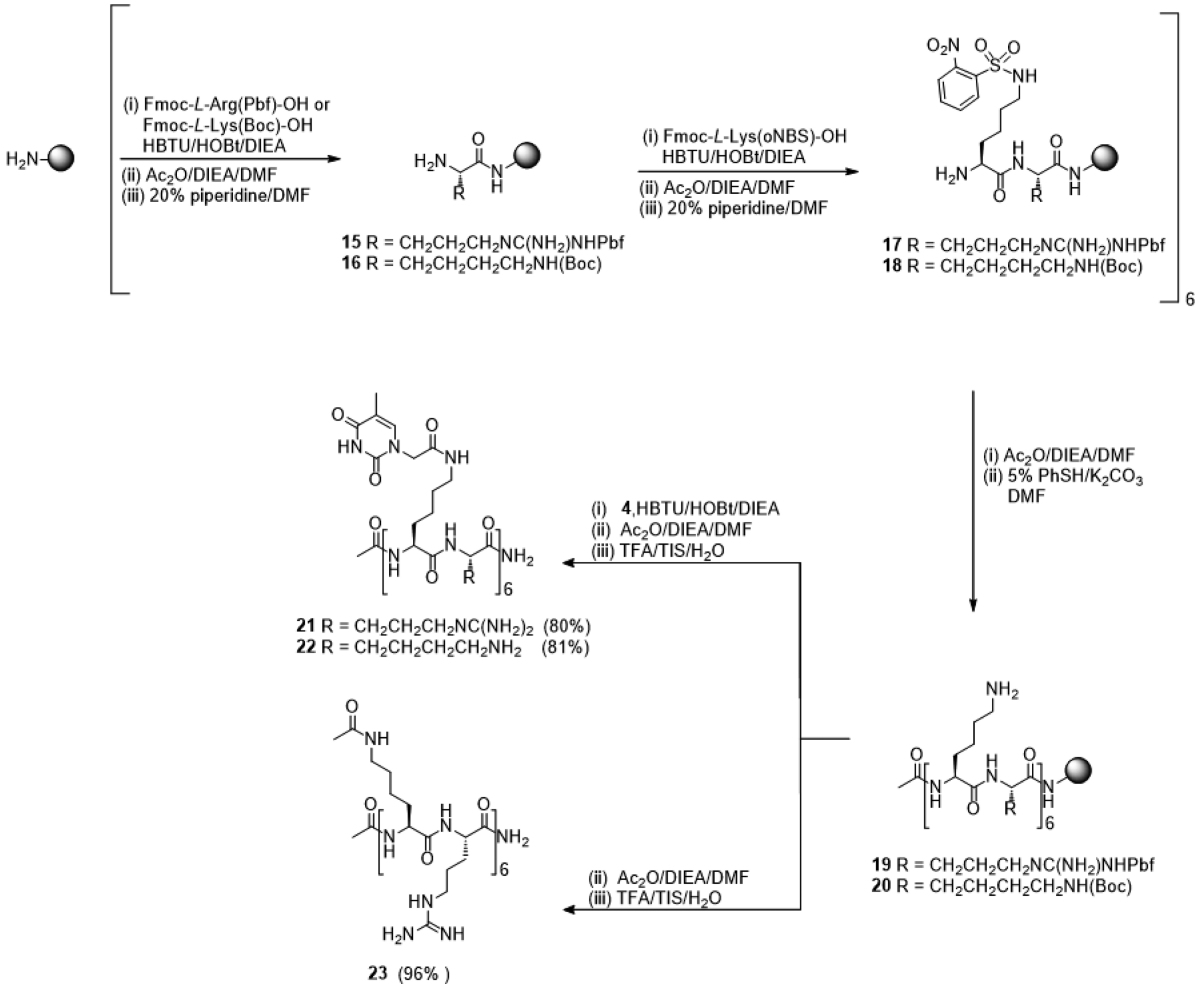

adopted fluorenylmethyloxycarbonyl (Fmoc), which is the most widely used for the solid phase peptide synthesis, because it is rapidly and quantitatively removed by mild base treatments of the peptide resin. As orthogonal protecting group, we employed 2-nitrobenzenesulfonyl (*o*NBS), that was first described by Fukuyama,[25] and then extensively adopted by Kessler and Miller

DOI: 10.1021/acs.joc.6b01829
J. Org. Chem. 2016, 81, 11612−11625

Scheme 3. Synthetic Route to FITC-Homonucleopeptide 26 and 27

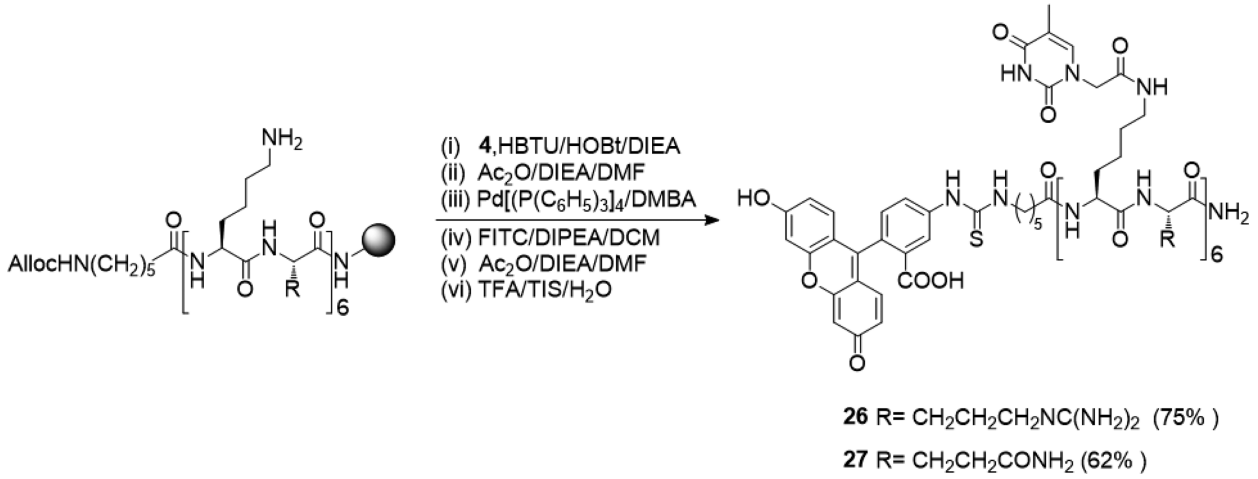

both for the selective alkylation of peptide on solid support and as a Fmoc alternative in the synthesis of unalkylated peptides.[26,27] *o*NBS is easily and quantitatively removed by treating the peptide resin with a K_2CO_3/thiophenol in DMF.[25] The switch of these two protecting groups led to the key intermediates X-L-Lys(Y)−OH, where X = Fmoc and Y = *o*NBS for the synthesis of homonucleopeptides, and X = *o*NBS and Y = Fmoc for the synthesis of heteronucleopeptides.

Fmoc-L-Lys(*o*NBS)-COOH was commercially available, while *o*NBS-L-Lys(Fmoc)-COOH[28] (**2**) was prepared in excellent yields by reacting the commercially available H-L-Lys(Fmoc)-COOH with *o*NBS-Cl in the presence of DIPEA as base (Scheme 1a). To functionalize the ε amino groups of L-Lys, thymine acetic acid (**4**) was synthesized as previously described (Scheme 1b), while bis-Boc protecting group was selected as strategy for the exocyclic amino functions of the cytosine (**7**), adenine (**10**), and guanine (**14**) nucleobases (Scheme 1c−e). The synthesis of the challenging Boc-protected nucleobase acetic acids (**7**, **10**, **14**) was carried out in solution modifying previously reported procedures.[29] In particular, we improved the yields of the alkylation step of the nucleobases by using Cs_2CO_3 instead of more harmful NaH, which is the base usually described for introducing the methyl bromoacetate moiety.[29] In addition, the displacement of the chlorine at the C-6 of the purine ring (**12**) with oxo-group (**13**) was performed with 1,4-diazabicyclo-[2.2.2]octane (DABCO) in the presence of potassium acetate and triethylamine in dioxane followed by treatment with a saturated aqueous solution of $NaHCO_3$, in order to ensure the full conversion of **12**-acetate intermediate into **13**. Compared to the previous protocols,[30] we significantly improved the methodology obtaining higher yields of nucleobase acetic acid derivatives and reducing the use of toxic reagents and solvents, such as volatile trimethylamine and DMF. In addition, cesium acetate that is usually described for the DABCO-based reaction[31] was replaced with the less expensive potassium acetate.

Synthesis of Homo and Heteronucleopeptides. As described in Scheme 2, the homo-oligomeric nucleopeptide consisting of a cationic backbone of 12 amino acid residues $(Lys\text{-}Arg)_6$ was assembled through progressive elongation reactions following standard solid-phase peptide synthesis protocols by using the aminomethyl polystyrene (AM-PS) resin functionalized with a Rink-amide linker, Fmoc-L-Lys(*o*NBS)−OH and Fmoc-L-Arg(Pbf)−OH. Although the introduction of a single *o*NBS protected amino acid has been previously described for backbone and side chain alkylations,[26] very few data are available on its employment as standard side chain protecting group. In our study, the full *o*NBS-protected sequence, was obtained with a high yield and purity, indicating that *o*NBS is an appropriate protecting group featuring high stability to reiterated cycles of Fmoc-deprotection and amino acid couplings.

At this step, the *N*-terminal function was acetylated and all the ε amino groups of L-Lys residues were simultaneously released using a saturated DMF solution of K_2CO_3 in the presence of thiophenol. To perform a complete *o*NBS deprotection, the treatment needs to be repeated three times using K_2CO_3 with a degree of purity ≥99.995%. The purity of K_2CO_3 has a tremendous impact on the efficiency of the deprotection process, indeed, when $K_2CO_3 \leq$ 99.995 was employed, we noticed an incomplete or no deprotection even increasing the reaction time and the number of treatments.

Next, the thymine residues previously functionalized with a methylene carbonyl linker (**4**) were introduced by one pot reaction via amide linkage in the presence of HBTU/HOBt for 3 h, affording hexathymine nucleopeptide **21** with impressive yield and purity as verified by HPLC analysis (see SI) and confirmed by MALDI-TOF MS (see SI).

The same one pot-strategy was adopted for the synthesis of peptide **23** (Scheme 2), consisting of 12 amino acid residues $(Lys\text{-}Arg)_6$, bearing acetyl groups instead of thymine at the ε position of L-Lys. Also, using this approach we prepared nucleopeptide **22** (Scheme 2), an analogue of **21** in which L-Arg residues were replaced by L-Lys. Both **22** and **23** were used as control to investigate the interactions driving the recognition process of **21** with its targets. In particular, for the synthesis of **22**, L-Arg was replaced by L-Lys, because it was the only alternative natural amino acid allowing to preserve a comparable solubility to **21**. Indeed, when L-Arg was substituted with L-Ala, L-Lys(Ac), and L-Ser the resulting nucleopeptides suffered of very low solubility in aqueous media, that hampered the binding studies (data not showed).

In addition two fluorescein isothiocyanate (FITC)-labeled nucleopeptides (**26** and **27**) were prepared adopting the same synthetic strategy (Scheme 3). The compound **26**, the (FITC)-labeled derivative of **21** was used to investigate the cellular uptake properties of our compounds. On the other hand, compound **27** was designed by replacing arginines with glutamines and used as negative control in the cell internalization experiment.

DOI: 10.1021/acs.joc.6b01829
J. Org. Chem. 2016, 81, 11612−11625

Scheme 4. Synthetic Route to Heteronucleopeptide 28

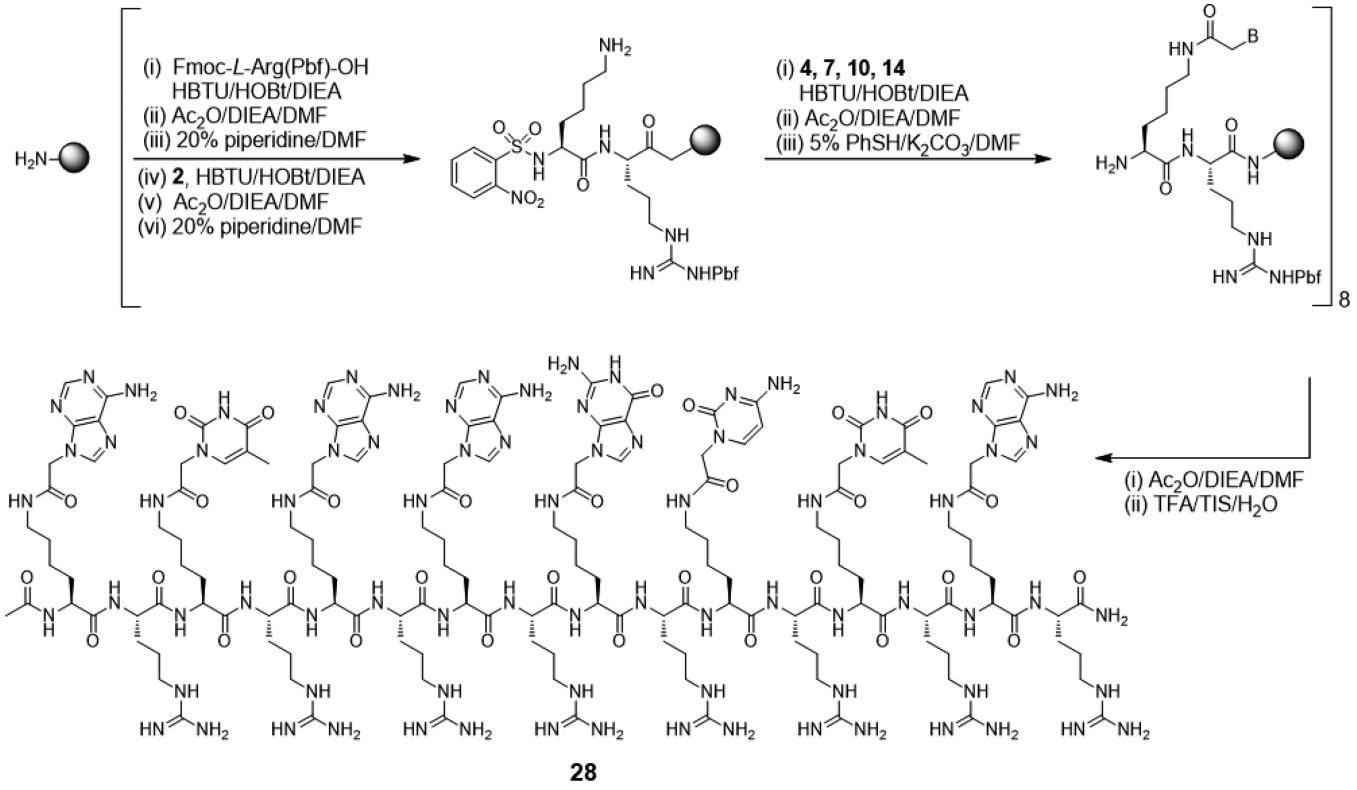

Glutamine is not considered an amino acid known to facilitate cell internalization, but it holds the capability to form hydrogen bonds that could confer an acceptable aqueous solubility for cell penetration experiments.

In both cases, the FITC moiety was linked to the supported nucleopeptides using an aminohexanoic spacer (Ahx) following a previously described procedure.[31] We selected allyloxycarbonyl (Alloc) as protecting group for the ε amine of the Ahx residue, based on the stability of Alloc to the *o*NBS deprotection conditions.[32]

The synthesis of heterosequence nucleopeptide **28** was achieved through a solid phase stepwise strategy exploiting *o*NBS-L-Lys(Fmoc)−OH (**2**) intermediate (Scheme 4). After Fmoc removal of the supported L-Arg, **2** was introduced following standard protocols for peptide synthesis. Next, the Fmoc-protecting group at the ε position of the supported *o*NBS-L-Lys was removed and the resulting free amine coupled with the suitable Boc-protected nucleobases (**4**, **7**, **10**, **14**) by HBTU/HOBt activation of the linker carboxy function. At this stage, the *o*NBS was removed from the nucleobase functionalized dimeric Lys-Arg building block applying the developed *o*NBS deprotection procedure described for the synthesis of homonucleopeptides. This enabled the growth of cationic nucleopeptide bearing mixed sequence by repetitive coupling cycles with (A) Fmoc-L-Arg(Pbf)−OH, (B) *o*NBS-L-Lys-(Fmoc)−OH, and (C) protected nucleobase acetic acid derivatives. Each coupling cycle was qualitatively monitored by Kaiser and 2,4,6-trinitrobenzenesulfonic acid (TNBS) tests,[33,34] and quantitatively verified by measurement of UV spectroscopic adsorption of the dibenzofulvene-piperidine adduct (≥98% yield). By using this strategy, we have synthesized **28**, containing the sequence ATAAGCTA, complementary to the seed region of the biologically relevant miRNA 21,[2] which was obtained in high yield (60% crude overall yield) and high degree of purity (≥90%) as characterized by RP-HPLC (see SI) and MALDI-TOF MS (see SI). The HPLC profile of crude **28** clearly indicates that reiterated *o*NBS deprotection treatments with K_2CO_3/thiophenol did not produce any significant side reactions during the synthesis of nucleopeptide **28**. These results promoted *o*NBS as valid alternative protecting group in the synthesis of peptide nucleic acid analogues along with Boc-protected nucleobases and unprotected thymine. All the final products, except **27**, displayed high degree of solubility in water without requiring the addition of organic solvents, such as ACN, MeOH, and/or DMSO. In the case of **27**, the addition of 5% DMSO was required to have a complete dissolution in water.

Conformational Analysis and Hybridization Properties. CD measurements were carried out for single stranded **21**−**23** and **28** at 6 μM concentration in 10 mM phosphate buffer (pH = 7.4) at rt. As shown in Figure 3, no significant CD signals in the region 205−300 nm were observed suggesting

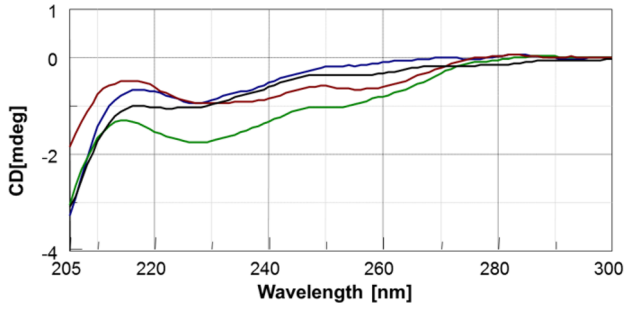

Figure 3. CD spectra of **21** (green), **22** (blue), **23** (red), and **28** (black).

DOI: 10.1021/acs.joc.6b01829
J. Org. Chem. 2016, 81, 11612−11625

that nucleopeptides **21**−**23** and **28** did not adopt any structural pre-organization.

Next, we started evaluating the DNA and RNA binding properties of **21** by hybridization experiments carried out with polydA and polyA single strands (ss), at 1:1 stoichiometry ratio. CD profiles of **21**/polydA and **21**/polyA hybrids revealed a remarkable change both in the intensity of the CD bands (hypochromic effect) and in their positions with respect to DNA and RNA ss, suggesting that recognition events occurred (Figure 4).

Consistent UV and CD melting temperature (Tm) measurements indicated that **21** binds the DNA and RNA targets, giving well-defined curves with higher Tm than those observed for natural duplexes (Table 1).

Since homopyrimidine/homopurine sequences are known to form triplex structures, CD spectra were also performed on the complex **21**/polydA in 2:1 stoichiometric ratio. CD profiles exhibited the presence of a negative dichroic band at 228 nm and the disappearance of the band at 248 nm observed in the duplex spectrum (Figure 5a), revealing the formation of triplex structure, as confirmed by CD tritation and Job's plot (Figure 5b and d). Two melting transitions at 25 and 40 °C were observed by UV experiment (Figure 5c).

In principle, the binding and the high thermal stability of cationic nucleopeptides toward DNA and RNA targets could arise from nonspecific electrostatic interactions between the nucleopeptide guanidinium residues and the target phosphate backbone.[18] To assess the role of the base-pairing into the hybridization process, we performed CD binding experiments with **23**, which bears acetyl groups instead of the thymine nucleobases. CD profiles of **23**/polydA and **23**/polyA turned out to be different from single stranded polydA and polyA and sum spectra, showing changes in signal intensities, probably due to the interactions between the cationic backbone of **23** and anionic nucleic acids. Mostly, the CD spectra of the hybrids **23**/polydA and **23**/polyA were different from CD profile of the hybrids **21**/polydA and **21**/polyA and from those of polydA and polyA, suggesting that ionic-directed binding occurred but the hybridization process was mainly controlled by base pairing rules (Figure 6). In addition, the dramatic changes observed in the CD profiles of hybrids involving **21**, those were not detected in the case of **23**, seem to indicate the involvement of both thymine and L-Arg residues in the target recognition mode.

Further investigations performed with the control nucleopeptide **22**, confirmed that the L-Arg residues are involved but did not drive the binding process. Indeed, comparison between **21**−**22**/polydA and **21**−**22**/polyA hybrid spectra (Figure 7) pointed out that L-Arg residues may provide extra interaction sites in RNA recognition process. Also, the resulting hybrids showed different thermal stability (Table 1). The reasons behind this different behavior of nucleopeptides bearing L-Arg (**21**) and L-Lys (**22**) require further studies.

Finally, the base-specific interaction of **21** with the complementary target (polydA) was confirmed by CD experiments carried out with **21**/noncomplementary $(T)_6$ and **21**/polydA.[35] As shown in Figure 8, CD spectra revealed that the DNA conformation was conserved when **21** was annealed with noncomplementary target, providing further evidence of the key role of thymines into the binding process.

Based on the recent data reporting as anti-miRNA approach the targeting of the seed region by 8mer oligonucleotide analogues,[5−8] we investigated the binding properties of the heteronucleopeptide **28**, consisting of the eight nucleobases sequence complementary to miR21 seed region. First, CD spectra and Tm of **28** were measured after hybridization with DNA and RNA (8 mer) complementary strands. Next, CD and Tm data were collected to evaluate the binding of **28** to the target miR21. CD spectrum of **28**/DNA duplexes showed hypochromic effect, a positive band at 270 nm accompanied by a negative band near 240 nm, typical of DNA/DNA duplexes, suggesting a conformational similarity of hybrid and natural DNA duplexes (Figure 9). In contrast, differences in the spectroscopic behavior can be observed for RNA duplexes, reflecting significant structural changes. When compared to the CD spectrum of RNA/RNA duplex, **28**/RNA hybrid exhibited a slight bathochromic shift of the positive band (from 264 to 270 nm) and the reduction of the weak negative band at 245 nm (Figure 9). These results clearly pointed out that **28** adopts different conformations in DNA and RNA hybrids, which could contribute to their different thermal stability.

As reported in Table 1, CD Tm measurements (for CD and UV melting profiles see SI) suggested that **28** formed thermostable duplexes with its DNA and RNA partners, exhibiting

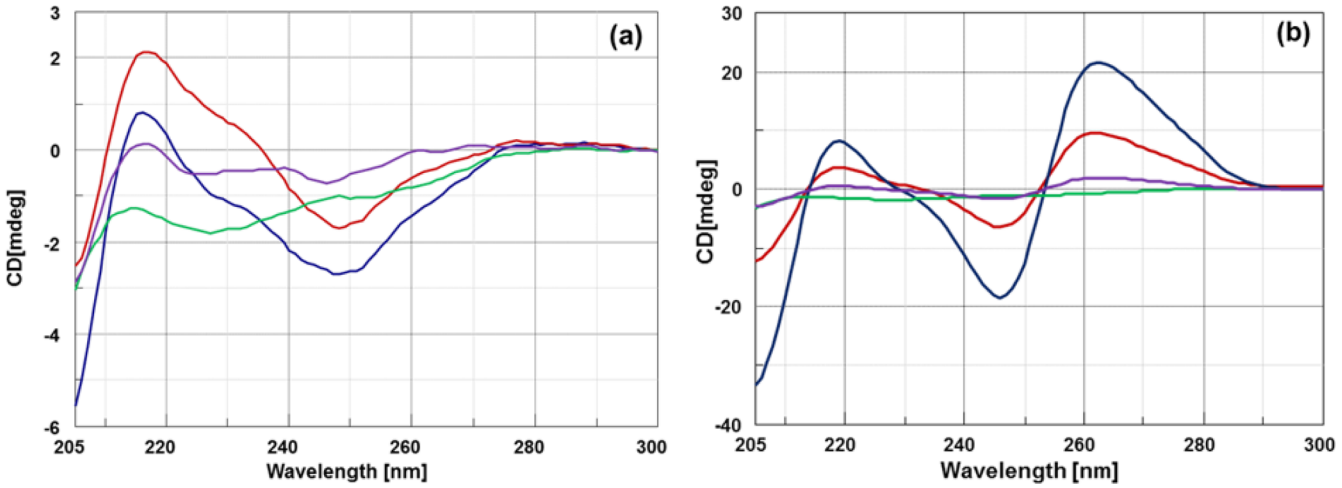

Figure 4. (a) CD spectra of polydA (red), **21**/polydA sum (blue), **21**(green), and **21**/polydA hybrid (violet) ; (b) CD spectra of polyA (red), **21**/polyA sum (blue), **21** (green), and **21**/polyA hybrid (violet).

DOI: 10.1021/acs.joc.6b01829
J. Org. Chem. 2016, 81, 11612−11625

Table 1. Tm Values of 21, 22, and 28 with Their Respective Nucleic Acid Targets[a]

hybrid duplexes	Tm (°C)	natural duplexes	Tm (°C)
tttttt (**21**)/ polydA	36	TTTTTT/polydA	25
tttttt (**21**)/ polyA	40	TTTTTT/polyA	35
tttttt (**22**)/ polydA	18		
tttttt (**22**)/ polyA	38		
ataagcta (**28**)/ 3′TATTCGAT-5′	35	5′-ATAAGCTA-3′/ 3′-TATTCGAT-5′	26
ataagcta (**28**)/ 3′-TATTAGAT-5′	30	5′-ATAAGCTA-3′/ 3′-TATTAGAT-5′	23
ataagcta (**28**)/ 3′-UAUUCGAU-5′	36	5′-AUAAGCUA-3′/ 3′-UAUUCGAU-5′	20
ataagcta (**28**)/ 3′-UAUUAGAU-5′	25	5′-AUAAGCUA-3′/ 3′-UAUUAGAU-5′	17
ataagcta (**28**)/ 3′AGUUGUAGUCAGAC**UAUUCGAU**-5′	39	5′-AUAAGCUA-3′/ 3′AGUUGUAGUCAGAC**UAUUCGAU**-5′	30

[a]Lowercase = nucleopeptide sequence; uppercase = natural nucleic acid sequence; **bold** = mir21 seed region sequence; red = mismatch.

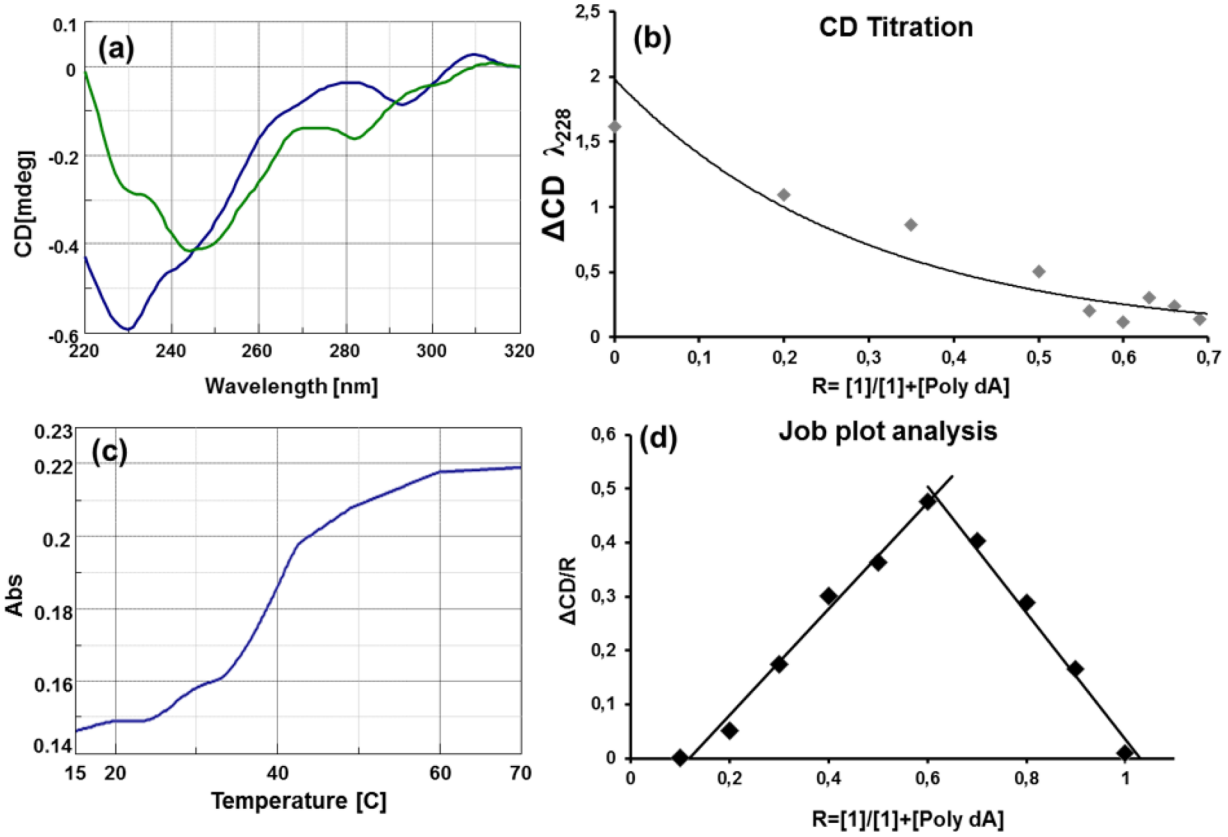

Figure 5. (a) CD spectra of **21**/polydA hybrid 1:1 stoichiometric ratio (green) and **21**/polydA hybrid 2:1 stoichiometric ratio (blue); (b) CD titration of the **21**/polydA hybrid from 0:1 to 2:1 stoichiometric ratio; (c) UV melting profile of **21**/polydA hybrid (2:1 stoichiometric ratio); (d) Job's plot of the **21**/polydA hybrid from 0:1 to 2:1 stoichiometric ratio.

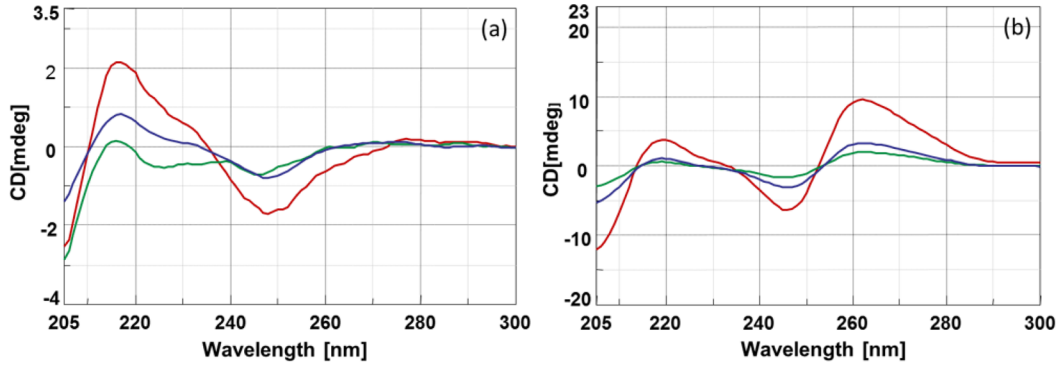

Figure 6. (a) CD spectra of polydA (red), **23**/polydA (blue), and **21**/polydA (green); (b) CD spectra of polyA (red), **23**/polyA (blue), and **21**/polyA (green).

DOI: 10.1021/acs.joc.6b01829
J. Org. Chem. 2016, 81, 11612−11625

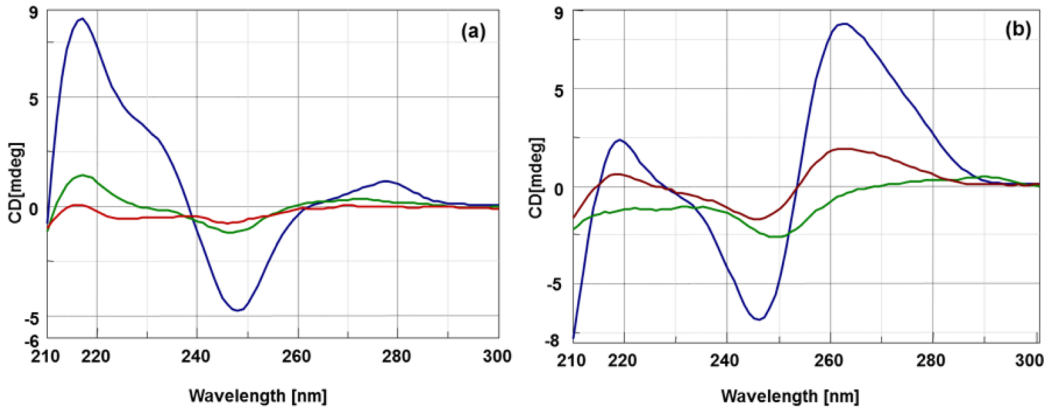

Figure 7. (a) CD spectra of polydA (blue), **22**/polydA (green), and **23**/polydA (red) hybrids; (b) CD spectra of polyA (blue), **22**/polyA (green), and **23**/polyA (red) hybrids.

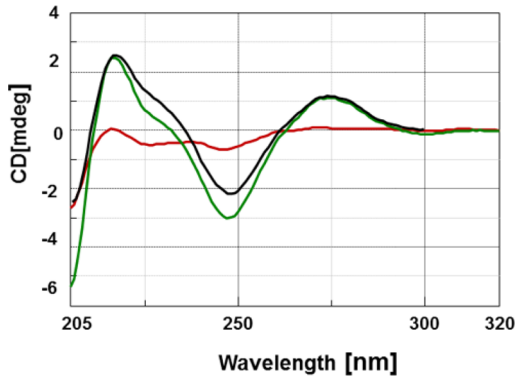

Figure 8. CD spectra of **21**/ polydA (red); T_6 DNA/polydA (black); and **21**/T_6 DNA (green).

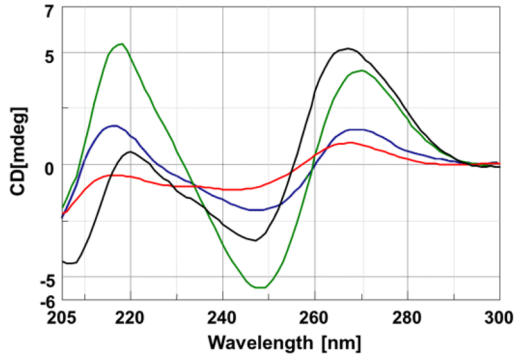

Figure 9. CD spectra of DNA/DNA (green) duplex vs **28**/DNA (blue) hybrid and RNA/RNA (black) duplex vs **28**/RNA (red) hybrid.

higher Tm than natural duplexes. Furthermore, the sequence specificity of **28** toward DNA and RNA targets was assessed by evaluating its ability to form stable duplexes with DNA and RNA having a single base mismatch (Table 1). The introduction of one mispairing, adenine instead than cytosine, destabilized by −5 °C and −11 °C for DNA and RNA duplexes, respectively, confirming the essential role of the base pairing in the duplex formation. The destabilization effect for mismatched RNA was significantly higher than mismatched DNA duplex indicating an inherently high sequence specificity of **28** toward RNA targets. Noteworthy, **28** showed excellent capabilities in discriminating mismatched targets, those in turn could reduce the off-target effects due to undesired sequence recognitions.

The ability of **28** to form stable duplex complex with RNA was confirmed by HPLC and ESI Q-TOF MS experiments. We were able to isolate **28**/RNA hybrid by RP-HPLC as a well-defined peak with a different retention time with respect to **28** and ss RNA, which was successfully characterized by ESI Q-TOF MS (Figure 10 and SI).

Furthermore, binding assay, Tm, and strand invasion experiments were carried out with **28** and miRNA target, to investigate its potential use in anti-miRNA approach using small oligomers complementary to the miRNA seed region. Interestingly, **28** could form stable complex with miRNA21 and mostly, to selectively displace RNA strand from the RNA/RNA duplex. In fact, 8-mer RNA/miR21 duplex CD spectrum changed in **28**/miR21 hybrid spectrum in 60 min when single strand **28** was added to preformed RNA/miR21 duplex solution (Figure 11a). Conversely, no changes were detected when the single strand **28** was added to the DNA/DNA duplex, even after 24 h (Figure 11b). This behavior opens new opportunities for the application of cationic nucleopeptides in the modulation of biogenesis and maturation of RNA molecules.

Biostability Studies. Considering the potential of nucleopeptides to become real therapeutics, we evaluated the stability of **21** when exposed to 90% human serum (Figure 12a). The inspections demonstrated that **21** starts to be degraded after 30 min, but it can be detected up to 120 min, which indicates a higher stability of **21** when compared the previously reported structural congeners.[29] To better investigate the proteolytic process that led to the degradation of **21**, we characterized by MALDI-TOF MS analyses the main breakdown products of nucleopeptide **21** (Figure 12b) at 30 min human serum incubation. The results pointed out that the proteolytic process is mediated by endopeptidase enzymes hydrolyzing the arginine peptide bonds. This observation can represent a useful information that could drive the optimization process of these new compounds toward the synthesis of more stable derivatives by introducing arginine surrogates or modification of the arginine amide bonds (i.e., *N*-methylation).

***In vitro* Cell Uptake.** Although, several studies correlated the enhancement of peptide cell permeability with the presence of arginine residues, to the best of our knowledge no investigation has been performed with arginine-rich nucleopeptides. To assess the capability of our nucleopeptides to penetrate into cells, LN229 glioblastoma cell line was incubated for 1 and 3 h with 50 μM concentration of **26** and processed for visualization by laser scanning confocal microscope. Moreover, **27** bearing

DOI: 10.1021/acs.joc.6b01829
J. Org. Chem. 2016, 81, 11612−11625

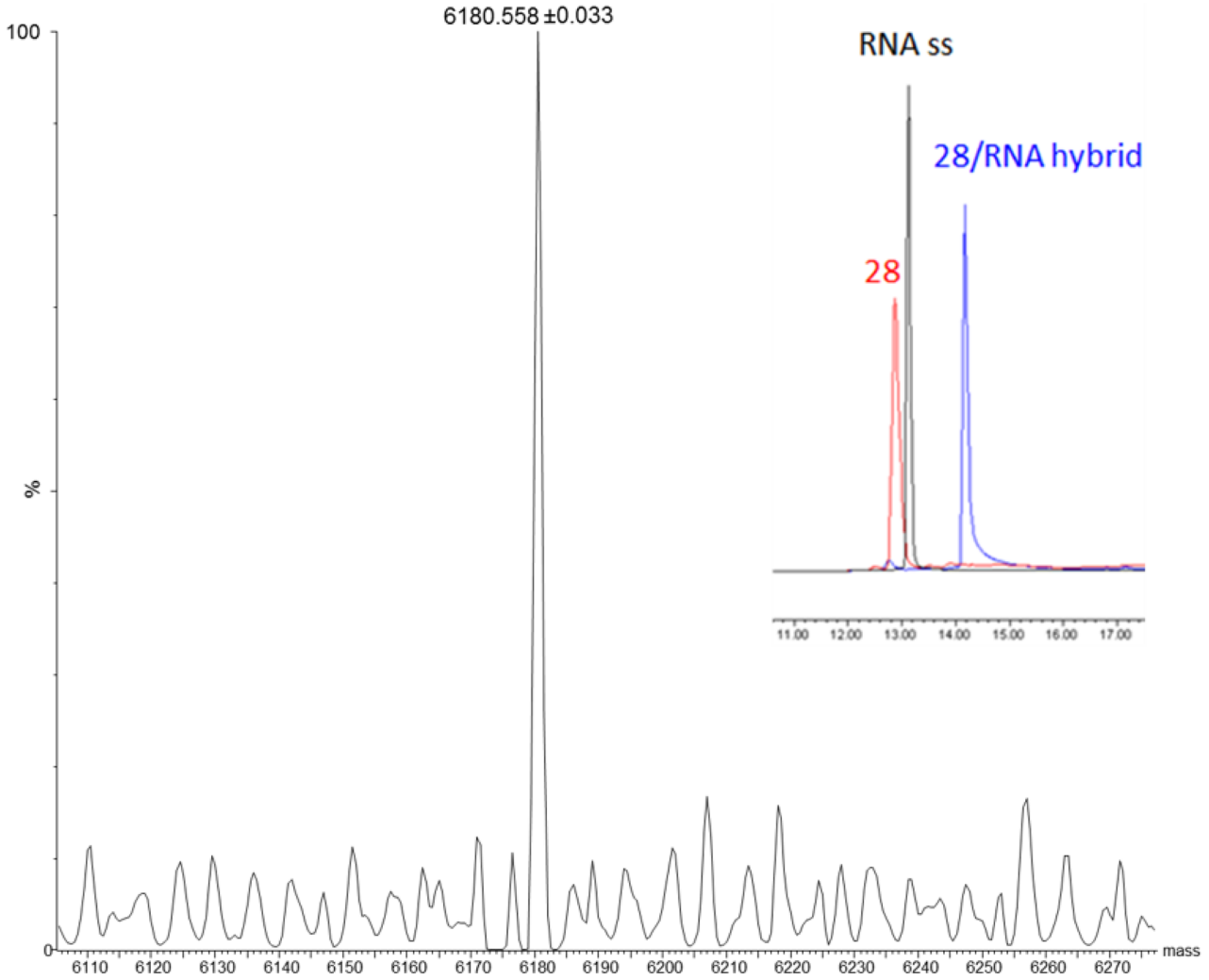

Figure 10. ESI-MS spectrum of **28**/RNA duplex; insert: analytical RP-HPLC profiles of **28** (red), ss RNA 8mer target (black), and **28**/RNA duplex (blue); 0 to 15% of ACN in 0.1 M TEAA aqueous buffer in 30 min.

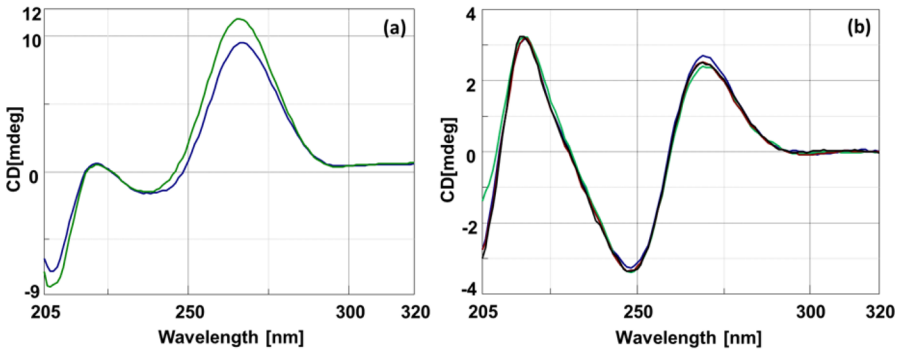

Figure 11. Strand invasion experiment of **28** in RNA/miR21 duplex; (a) RNA duplex (green), addition of **28** in RNA duplex (60 min, blue). (b) Strand invasion experiment of **28** in DNA duplex; DNA duplex (green), addition of **28** in DNA duplex (red 60 min, black 120 min, and blue 24 h).

Gln residues instead of arginines was tested to assess the role of arginines in the cell internalization process of nucleopeptides. As shown in Figure 13, for compound **26**, the green fluorescence was observed for both tested time intervals. In particular, at 1 h the **26**-treated LN299 cells showed a strong nuclear localization indicating that our nucleopeptide could cross nucleus membrane without the assistance of a nuclear localization signal peptides (NLS). Interestingly, after 3 h, a diffusion of the fluorescence signal was observed, probably triggered by interaction of **26** with polyA targets, those are abundantly distributed also in the cell cytoplasm. As expected, no cellular uptake was observed for **27**, confirming that arginine is the essential component for cell penetration.

■ CONCLUSIONS

In conclusions, the synergistic use of peptide and nucleic acid chemistry led to the development of a powerful strategy for the facile solid-phase synthesis of homo- and heterocationic

DOI: 10.1021/acs.joc.6b01829
J. Org. Chem. 2016, 81, 11612−11625

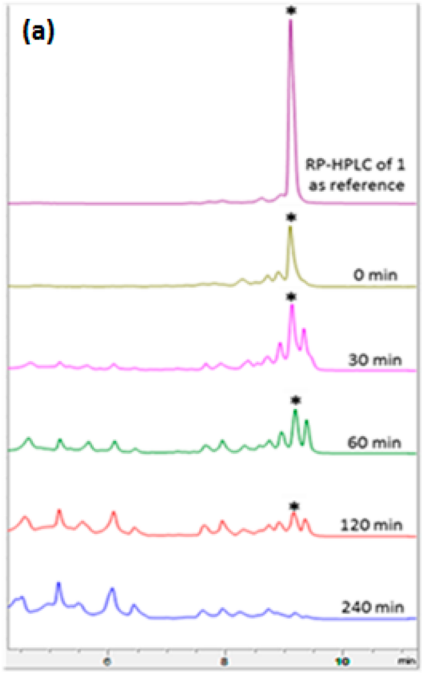

(b)

retention time	M.W. fragments
8.90	805.36[a] 1255.66[b]
9.08	1705.82[c] 2157.04[d] 2607.31[e] 2762.48[f]
9.30	2157.04[d] 2607.35[e]

[a]Ac-K(T)RK(T)-COOH
[b]Ac-K(T)RK(T)RK(T)-COOH
[c]Ac-K(T)RK(T)RK(T)RK(T)-COOH
[d]Ac-K(T)RK(T)RK(T)RK(T)RK(T)-COOH
[e]Ac-K(T)RK(T)RK(T)RK(T)RK(T)RK(T)-COOH
[f]Ac-K(T)RK(T)RK(T)RK(T)RK(T)RK(T)R-$CONH_2$

Figure 12. (a) RP-HPLC analysis of **21** in 90% human serum at 37 °C at different times; 0 to 90% ACN (0.1% TFA) in water (0.1% TFA) over 30 min. The HPLC profile shows the results of one representative experiment out of at least three independent ones. (b) MALDI-TOF MS analyses of the main breakdown products of **21** after 30 min human serum incubation.

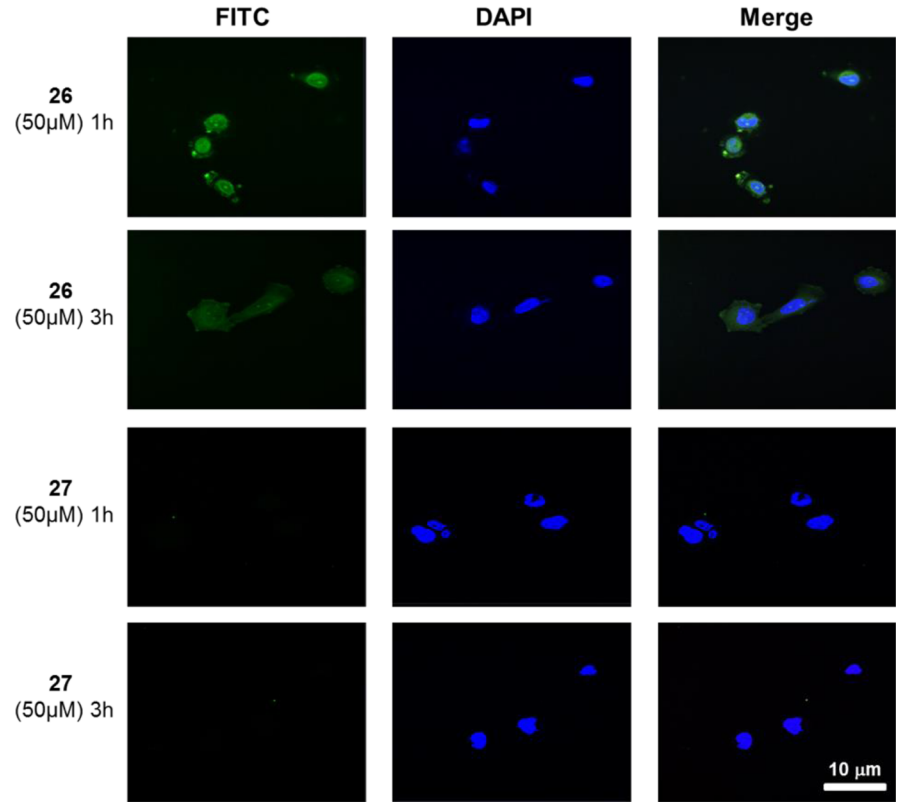

Figure 13. Laser scanning confocal microscope images of the distribution of FITC-nucleopeptides **26** and **27** (50 μM) inside LN229 Glioblastoma cell line at 1 and 3 h. The nuclei were stained with DAPI (blue). Images were obtained by an LSM-410 Zeiss confocal microscope. Nucleopeptide **27** was employed as negative control.

nucleopeptides with high yield and purity. These new chemotypes exhibited intriguing advantageous properties in terms of solubility in aqueous medium, thermodynamic stability, and sequence specificity for RNA and DNA, with effective mismatch discrimination especially for RNA. In order to translate these promising results into an effective biological application, human serum stability, and cellular uptake studies provided preliminary but still solid evidence that our nucleopeptides feature acceptable

DOI: 10.1021/acs.joc.6b01829
J. Org. Chem. 2016, 81, 11612−11625

serum stability and ability to efficiently reach cellular compartments. We anticipate that our synthetic method can be suitable for a variety of structural modifications of nucleopeptides, such as introduction of D- and L-, α-, and β-amino acids, N-alkylation, cyclization, and replacements of nucleobases. This will finally allow for a fine optimization of these chemotypes to deliver their full potential as new gene modulators.

EXPERIMENTAL SECTION

***o*NBS-L-Lys(Fmoc)OH (2).** A solution of H-L-Lys(Fmoc)−OH (1.0 g, 2.72 mmol, 1 equiv) and DIPEA (4.40 mL, 25.0 mmol, 9.2 equiv) in THF/H_2O (100 mL, 1:1) was cooled down at 0 °C in an ice bath then a solution of 2-nitrobenzensulfonyl chloride (0.66 g, 2.99 mmol, 1.1 equiv) in THF (3 mL) was added dropwise and the reaction allowed to stir at rt for 1 h. The organic solvent was evaporated under reduced pressure and the remaining solution acidified to pH 1 with HCl 0.1 N. The aqueous phase was then extracted with EtOAc (3 × 60 mL), the combined organic layers were dried with anhydrous Na_2SO_4, filtered, and concentrated *in vacuo*. The crude mixture was purified by silica gel chromatography (DCM/MeOH 95:5; 1% AcOH) and fractions of interest were collected to give **2** (1.46 g, 97%) as white solid. ^{1}H NMR (400 MHz, DMSO): δ 8.48 (bs, 1 H), 8.06−8.04 (m, 1H), 7.94−7.92 (m, 1H), 7.88−7.86 (m, 2H), 7.83−7.81 (m, 2H), 7.70−7.63 (m, 2H), 7.40 (t, J = 7.2 Hz, 2H), 7.33 (t, J = 7.2 Hz, 2H), 7.24 (m, 1H), 4.39−4.21 (m, 3 H), 3.88−3.84 (m, 1H), 2.94−2.89 (m, 2H), 1.75−1.58 (m, 2H), 1.34−1.10 (m, 4H) ppm. ^{13}C NMR (400 MHz, DMSO): δ 172.7, 156.1, 147.3, 144.0, 140.8, 134.0, 133.4, 132.5, 129.9, 127.6, 127.1, 125.2, 124.2, 120.1, 62.3, 55.9, 46.9, 31.5, 28.7, 22.4, 21.1 ppm. HRMS: Calculated: 554.19571 for $C_{27}H_{28}N_3O_8S$ [M+H$^+$]. Found: 554.15875.

2-(5-Methyl-2,4-dioxo-3,4-dihydropyrimidin-1(2*H*)-yl)acetic Acid (4). Thymine (2 g, 15.86 mmol, 1 equiv) was dissolved in a solution of KOH (3.42 g, 61.07 mmol, 3.8 equiv) in water (10 mL) and the reaction was allowed to stir at 50 °C for 5 min. After complete dissolution of the reactants, a solution of bromoacetic acid (3.30 g, 23.80 mmol, 1.5 equiv) in water (5 mL) was added dropwise and the mixture stirred at 50 °C overnight. The reaction was cooled down in ice bath and pH slowly acidified with HCl 4N. The desired product **7** (2.19 g, 75%) was obtained by filtration as white solid and used without any further purification. R_f = 0.12 (DCM/MeOH, 75:25; 1% AcOH). R_f = 0.15 (DCM/MeOH, 75:25; 1.5% AcOH). ^{1}H NMR (400 MHz, DMSO): δ 13.06 (bs), 11.33 (s, 1 H), 7.48 (s, 1H), 4.36 (s, 2H), 1.75 (s, 3H). ^{13}C NMR (400 MHz, DMSO): δ 169.71, 164.42, 151.04, 141.85, 108.41, 48.47, 11.96 ppm. HRMS: Calculated: 185.05623 for $C_7H_8N_2O_4$ [M+H$^+$]. Found: 185.05559.

Methyl 2-{4-[Bis(*tert*-butoxycarbonyl)amino]-2-oxopyrimidin-1(2*H*)- yl}acetate (6). Compound **5** (1.70 g, 5.46 mmol, 1 equiv)[33] and dry Cs_2CO_3 (1.96 g, 6.01 mmol, 1.1 equiv) were suspended in dry CH3CN (15 mL) and left to stir at 0 °C for 10 min under Ar atmosphere. A solution of BrCH2CO2Me (0.569 mL, 6.01 mmol, 1.1 equiv) in dry CH_3CN (3 mL) was added dropwise and the reaction was allowed to stir at room temperature for 2 h. The reaction was quenched with H_2O (50 mL) and extracted with EtOAc (3 × 60 mL), the combined organic layers were then washed with NaCl s.s., dried over anhydrous Na_2SO_4, and the solvent evaporated under reduced pressure. The crude was purified by flash chromatography on silica gel (DCM/MeOH, 97:3; 0.5% AcOH) to give **6** (1.82 g, 87%) as pale yellow solid. R_f = 0.45 (DCM/MeOH, 96:4; 0.5% AcOH). ^{1}H NMR (400 MHz, CDCl3): δ 7.49 (d, J = 7.4 Hz, 1H), 7.09 (d, J = 7.4 Hz, 1H), 4.56 (s, 2H), 3.76 (s, 3H), 1.54 (s, 18H). ^{13}C NMR (400 MHz, CDCl3): δ 167.81, 163.01, 154.90, 149.55, 148.12, 96.67, 85.18, 52.92, 50.97, 27.80 ppm. HRMS: Calculated: 384.17708 for $C_{17}H_{26}N_3O_7$ [M+H$^+$]. Found: 384.17624.

2-{4-[Bis(*tert*-butoxycarbonyl)amino]-2-oxopyrimidin-1(2*H*)-yl}acetic acid (7). Compound **6** (1.5 g, 3.91 mmol, 1 equiv) was dissolved in THF (16 mL) and placed in an ice bath under vigorous stirring. Sodium hydroxide (188 mg, 4.69 mmol, 1.2 equiv) in H_2O (2.35 mL, 2 N) was then added dropwise and the reaction was allowed to stir at room temperature for 30 min. The mixture was cooled to 0 °C, diluted with 70 mL of EtOAc and the pH neutralized by adding 0.78 mL of HCl aq. 1 N dropwise. The pH was finally adjusted to 2−3 by dropping HCl aq. 0.1 N and the aqueous layer extracted with EtOAc (5 × 70 mL). The combined organic layers were then washed with a small aliquot of saturated NaCl aq., dried with anhydrous Na_2SO_4, filtered, and concentrated under reduced pressure to give the desired compound **7** (1.37 mg, 95%) as white solid. R_f = 0.35 (DCM/MeOH, 96:4; 0.5% AcOH). ^{1}H NMR (400 MHz, DMSO): 13.16 (s, 1H), 8.13 (d, J = 7.2 Hz, 1H), 6.83 (d, J = 7.2 Hz, 1H), 4.56 (s, 2H), 1.49 (s, 18H) ppm. ^{13}C NMR (400 MHz, DMSO): δ 169.11, 162.07, 154.14, 151.16, 149.23, 95.44, 84.56, 50.83, 27.25 ppm. HRMS: Calculated: 370.16143 for $C_{16}H_{23}N_3O_7$ [M+H$^+$]. Found: 370.16046.

Methyl 2-{6-[Bis(*tert*-butoxycarbonyl)amino]-9*H*-purin-9-yl}-acetate (9). Compound **8** (1.75 g, 5.22 mmol, 1 equiv)[33] and dry Cs_2CO_3 (1.87 g, 5.74 mmol, 1.1 equiv) were suspended in dry CH_3CN (17 mL) and left to stir at 0 °C for 10 min under Ar atmosphere. A solution of $BrCH_2CO_2Me$ (0.543 mL, 5.74 mmol, 1.1 equiv) in dry CH_3CN (3.5 mL) was added dropwise and the reaction was allowed to stir at room temperature for 1 h. The reaction was quenched with H_2O (50 mL) and extracted with EtOAc (3 × 50 mL), the combined organic layers were then washed with NaCl s.s., dried over anhydrous Na_2SO_4, and the solvent was evaporated under reduced pressure. The crude was purified by flash chromatography on silica gel (EtOAc/hexane, 75:25) to give **9** (1.77 g, 83%) as off-white foam. R_f = 0.30 (DCM/MeOH, 98:2). ^{1}H NMR (400 MHz, $CDCl_3$): δ 8.84 (s, 1 H), 8.13 (s, 1 H), 5.06 (s, 2 H), 3.80 (s, 3 H), 1.43 (s, 18 H) ppm. ^{13}C NMR (400 MHz, $CDCl_3$): δ 167.28, 153.50, 152.43, 150.61, 150.42, 145.06, 128.44, 83.92, 53.22, 44.32, 27.88 ppm. HRMS: Calculated: 408.18831 for $C_{18}H_{26}N_5O_6$ [M+H$^+$]. Found: 408.18732.

2-{6-[Bis(*tert*-butoxycarbonyl)amino]-9*H*-purin-9-yl}acetic acid (10). Compound **9** (1.5 g, 3.68 mmol, 1 equiv) was dissolved in THF (15 mL) and placed in an ice bath under vigorous stirring. Sodium hydroxide (177 mg, 4.42 mmol, 1.2 equiv) in H_2O (2.2 mL, 2 N) was then added dropwise and the reaction was allowed to stir at room temperature for 30 min. The mixture was cooled to 0 °C, diluted with 80 mL of EtOAc and the pH neutralized by adding 0.74 mL of HCl aq. 1 N dropwise. The pH was finally adjusted to 2−3 by dropping HCl aq. 0.1 N and the aqueous layer extracted with EtOAc (6 × 80 mL). The combined organic layers were then washed with a small aliquot of saturated NaCl aq., dried with anhydrous Na_2SO_4, filtered, and concentrated under reduced pressure to give the desired compound **10** (1.38 mg, 95%) as white and fluffy solid. R_f = 0.38 (DCM/MeOH, 88:12; 0.5% AcOH). ^{1}H NMR (400 MHz, DMSO): δ 13.43 (s, 1H), 8.84 (s, 1H), 8.61 (s, 1H), 5.15 (s, 2H), 1.38 (s, 18H) ppm. ^{13}C NMR (400 MHz, DMSO): δ 168.86, 153.30, 151.59, 150.01, 149.04, 147.36, 127.40, 83.33, 44.52, 27.28 ppm. HRMS: Calculated: 394.17266 for $C_{17}H_{23}N_5O_6$ [M+H$^+$]. Found: 394.17172.

Methyl 2-{2-[Bis(*tert*-butoxycarbonyl)amino]-6-chloro-9*H*-purin-9-yl}acetate (12). Compound **11** (1.9 g, 5.14 mmol, 1 equiv)[33] and dry Cs_2CO_3 (1.84 g, 5.65 mmol, 1.1 equiv) were suspended in dry CH_3CN (20 mL) and left to stir at 0 °C for 10 min under Ar atmosphere. A solution of $BrCH_2CO_2Me$ (0.535 mL, 5.65 mmol, 1.1 equiv) in dry CH_3CN (4 mL) was added dropwise and the reaction was allowed to stir at room temperature for 1 h. The reaction was quenched with H_2O (60 mL) and extracted with EtOAc (3 × 60 mL), the combined organic layers were then washed with NaCl s.s., dried over anhydrous Na_2SO_4, and the volatiles evaporated to dryness *in vacuo*. The crude was purified by flash chromatography on silica gel (DCM/MeOH, 100:1; 0.5% AcOH) to give **12** (2.04 g, 85%) as white solid. R_f = 0.25 (DCM/MeOH, 100:1; 0.5% AcOH). ^{1}H NMR (400 MHz, $CDCl_3$): δ 8.21 (s, 1H), 5.04 (s, 2H), 3.79 (s, 3H), 1.41 (s, 18H) ppm. ^{13}C NMR (400 MHz, $CDCl_3$): δ 166.87, 152.91, 152.26, 151.44, 150.56, 146.46, 129.68, 83.85, 53.26, 44.57, 27.92 ppm. HRMS: Calculated: 442.14934 for $C_{18}H_{24}ClN_5O_6$ [M+H$^+$]. Found: 442.14832.

Methyl 2-{2-[Bis(*tert*-butoxycarbonyl)amino]-6-oxo-1*H*-purin- 9(6*H*)-yl}acetate (13). Compound **12** (1.35 g, 3.06 mmol, 1 equiv) and CH_3COOK (901 mg, 9.18 mmol, 3 equiv) were suspended in 1,4-dioxane (40 mL) and Et_3N (1,28 mL, 9.18 mmol, 3 equiv)

DOI: 10.1021/acs.joc.6b01829
J. Org. Chem. 2016, 81, 11612−11625

was added. The so obtained suspension was sonicated for 30 min at room temperature then DABCO (34 mg, 0.306 mmol, 0.1 equiv) was added portionwise while vigorously stirring and the mixture allowed to stir at room temperature overnight. Saturated $NaHCO_3$ aq. (30 mL) was added and the mixture vigorously stirred for other 30 min. The suspension was poured in a separatory funnel and washed with EtOAc (50 mL), the organic phase was back-extracted with further saturated $NaHCO_3$ aq. aliquots (2 × 15 mL). The combined aqueous layers were then placed in ice bath, neutralized dropwise with HCl 1 N and then adjusted to pH 2−3 by dropping HCl 0.1 N. The solution was extracted with EtOAc (4 × 100 mL) and the combined organic phases were dried with anhydrous Na_2SO_4, filtered, and concentrated *in vacuo* to give a white solid which was triturated in a mixture of hexane/ethylic ether 8:2 (20 mL). The suspension was filtered and the desired product **13** was obtained as white solid (1.24 g, 93%). R_f = 0.33 (hexane/EtOAc, 1:9). ^{1}H NMR (400 MHz, $CDCl_3$): δ 11.39 (s, 1H), 7.72 (s, 1H), 4.79 (s, 2H), 3.75 (s, 3H), 1.53 (s, 18H) ppm. ^{13}C NMR (400 MHz, $CDCl_3$): δ 167.17, 155.96, 149.10, 148.56, 146.49, 139.53, 120.96, 86.28, 53.01, 44.50, 27.70 ppm. HRMS: Calculated: 424.18332 for $C_{18}H_{26}N_5O_7$ [M+H$^+$]. Found: 424.18222.

2-{2-[Bis(*tert*-butoxycarbonyl)amino]-6-oxo-1*H*-purin-9(6*H*)-yl}acetic Acid (14). Compound **13** (1.1 g, 2.60 mmol, 1 equiv) was dissolved in THF (12 mL) and placed in an ice bath under a vigorous stirring. Sodium hydroxide (229 mg, 5.72 mmol, 2.2 equiv) in H_2O (2.9 mL, 2 N) was then added dropwise and the reaction was allowed to stir at room temperature for 1 h. The mixture was cooled to 0 °C, diluted with 80 mL of EtOAc, and the pH neutralized by adding 3.2 mL of HCl aq. 1 N dropwise. The pH was finally adjusted to 2−3 by dropping HCl aq. 0.1 N and the aqueous layer extracted with EtOAc (6 × 80 mL). The combined organic layers were then washed with a small aliquot of saturated NaCl aq., dried with anhydrous Na_2SO_4, filtered, and concentrated under reduced pressure to give the desired compound **14** (926 mg, 87%) as white solid. R_f = 0.40 (DCM/MeOH, 9:1, 1.5% AcOH). ^{1}H NMR (400 MHz, DMSO): δ 12.83 (s, 1H), 8.08 (s, 1H), 4.92 (s, 2H), 1.37 (s, 18H) ppm. ^{13}C NMR (400 MHz, DMSO): δ 168.90, 156.96, 148.75, 148.20, 145.15, 141.91, 122.23, 83.79, 44.76, 27.36 ppm. HRMS: Calculated: 410.2 for $C_{17}H_{24}N_5O_7$ [M+H$^+$]. Found: 410.166782; Calculated: 410.16757.

*Nucleopeptides **21**−**23**.* A Rink Amide AM-PS resin (50 mg, 0.48 mmol/g) was swelled in a mixture of DCM/DMF 1:1 over 30 min and washed with DCM and DMF three times. Fmoc protecting group was removed treating with 20% (v/v) piperidine solution in DMF (1 × 5 min; 1 × 25 min). The following amide couplings were carried out using 4 equiv (according to the initial loading of the resin) of the Fmoc-protected L-amino acids. To a prestirred solution of Fmoc-L-Arg(Pbf)−OH (for compounds **21** and **23**) (62.3 mg, 4 equiv) or Fmoc-L-Lys(Boc)−OH (44.98 mg, 4 equiv) (for peptide **22**) (45.0 mg, 4 equiv) with HBTU (36.4 mg, 4 equiv) and HOBT·H_2O (14.7 mg, 4 equiv) in DMF (1.0 mL), DIPEA (33.4 μL, 8 equiv) was added and the solution poured to the preswollen resin. The mixture was gently shaken for 2 h at rt and then washed with DMF (3 × 1 min) and DCM (3 × 1 min). Subsequently, to cap the remaining free amines the resin was treated with a solution of Ac_2O (4.5 μL, 2 equiv) and DIPEA (8.4 μL, 2 equiv) in DMF (1 mL) and then shaken for 10 min. Elongation of the linear peptide sequence was obtained by iterative cycles of the aforementioned Fmoc deprotections and coupling reactions with Fmoc-L-Lys(*o*NBS)−OH and Fmoc-L-Arg(Pbf)−OH. Completion of these steps were qualitatively monitored by Kaiser ninhydrine and TNBS test and quantitatively ascertained by Fmoc UV spectroscopic measurements. After the last Fmoc removal, *N*-terminal was acetylated by treatment with a mixture of Ac_2O (4.5 μL, 2 equiv) and DIPEA (8.4 μL, 2 equiv) in DMF (1 mL) over 30 min. One-pot *o*-nitrobenzenesulfonyl- (*o*NBS) removal on lysine side chains was obtained by adding 1.5 mL of a centrifuged 5% (v/v) solution of thiophenol in DMF, previously saturated with 2 eq. of K_2CO_3 (relative to thiophenol), to the resin (3 × 10 min).

*Nucleopeptide **21,22**.* Final coupling was performed using 3 equiv of nucleobase derivative, HBTU, and HOBt, and 6 equiv of DIPEA relative to each lysine ε amino group. Thymin-1-yl-acetic acid (compound **5**, 79.6 mg, 3 equiv), HBTU (163.7 mg, 3 equiv) and HOBt (66.2 mg, 3 equiv) were dissolved in DMF (1.5 mL) then DIPEA (150.5 μL, 6 equiv) was added and the resulting solution poured to the resin. The mixture was shaken at rt for 8 h. The unreacted free amines were capped with a solution of Ac_2O (27.2 μL, 2 eq. relative to each free amine) and DIPEA (50.2 μL, 2 equiv) in DMF (1 mL) over 10 min.

*Nucleopeptide **23**.* Acetylation of was achieved using 2 equiv of Ac_2O and DIPEA relative to each lysine ε amino group. A prestirred solution of Ac_2O (27.2 μL, 2 equiv) and DIPEA (50.2 μL, 2 equiv) in DMF (1 mL) was added and the resin shaked for 30 min.

*Nucleopeptides **26,27**.* A Rink Amide AM-PS resin (50 mg, 0.48 mmol/g) was swelled in a mixture of DCM/DMF 1:1 over 30 min and washed with DCM and DMF three times. Fmoc protecting group was removed treating with 20% (v/v) piperidine solution in DMF (1 × 5 min; 1 × 25 min). The following amide couplings were carried out using 4 equiv (according to the initial loading of the resin) of the Fmoc-protected L-amino acids. To a prestirred solution of Fmoc-L-Arg(Pbf)−OH (for compound **26**) (62.3 mg, 4 equiv) or Fmoc-L-Gln(Trt)−OH (58.6 mg, 4 equiv) (for compound **27**) with HBTU (36.4 mg, 4 equiv) and HOBt*H_2O (14.7 mg, 4 equiv) in DMF (1.0 mL), DIPEA (33.4 μL, 8 equiv) was added and the solution was poured to the preswollen resin. The mixture was gently shaken for 2 h at rt and then washed with DMF (3 × 1 min) and DCM (3 × 1 min). Subsequently, to cap the remaining free amines the resin was treated with a solution of Ac_2O (4.5 μL, 2 equiv) and DIPEA (8.4 μL, 2 equiv) in DMF (1 mL) and then shaken for 10 min. Elongation of the linear peptide sequence was obtained by iterative cycles of the aforementioned Fmoc deprotections and coupling reactions with Fmoc-L-Lys(*o*NBS)−OH and Fmoc-L-Arg(Pbf)−OH. Completion of these steps were qualitatively monitored by Kaiser ninhydrine and TNBS test and quantitatively ascertained by Fmoc UV spectroscopic measurements. After Fmoc removal, the N-terminal amino group was coupled with Aloc-Ahx−OH (mg, 4 equiv) in the presence of HBTU (36.4 mg, 4 equiv) and HOBt*H_2O (14.7 mg, 4 equiv) in DMF (1.0 mL) and DIPEA (33.4 μL, 8 equiv) as base. The mixture was gently shaken for 2 h at rt and then washed with DMF (3 × 1 min) and DCM (3 × 1 min). Subsequently, to cap the remaining free amines the resin was treated with a solution of Ac_2O (4.5 μL, 2 equiv) and DIPEA (8.4 μL, 2 equiv) in DMF (1 mL) and then shaken for 10 min. One-pot *o*-nitrobenzenesulfonyl- (*o*NBS) removal on lysine side chains was obtained adding 1.5 mL of a centrifuged 5% (v/v) solution of thiophenol in DMF, previously saturated with 2 equiv of K_2CO_3 (relative to thiophenol) to the resin (3 × 10 min). The coupling of thimine residues was performed using 3 equiv of nucleobase derivative, HBTU, and HOBt, and 6 equiv of DIPEA relative to each lysine ε amino group. Thymin-1-yl-acetic acid (compound **5**, 79.6 mg, 3 equiv), HBTU (163.7 mg, 3 equiv), and HOBt (66.2 mg, 3 equiv) were dissolved in DMF (1.5 mL) then DIPEA (150.5 μL, 6 equiv) was added and the resulting solution was poured to the resin. The mixture was shaken at rt for 3 h. The unreacted free amines were capped with a solution of Ac_2O (27.2 μL, 2 equiv relative to each free amine) and DIPEA (50.2 μL, 2 equiv) in DMF (1 mL) over 10 min. At this step the allyloxy protecting group of Ahx was removed by treating the resin with tetrakis(triphenyphosphine)-palladium(0) (12.0 mg, 0.1 equiv) and *N*,*N*′-dimethylbarbituric acid (156.1 mg, 10 equiv) in DCM/DMF (3:1, 3 mL) for 1 h at rt under nitrogen atmosphere, and the reaction was repeated again. After the resin was washed with DMF (3 × 1 min) and DCM (3 × 1 min), fluorescein-5- isothiocyanate (FITC) (233.6 mg, 6 equiv) and DIEA (209 μL, 12 equiv) in DMF (2 mL) were added and the reaction mixture was shaken 12 h in the dark. The unreacted free amines were capped with a solution of Ac_2O (27.2 μL, 2 eq. relative to each free amine) and DIPEA (50.2 μL, 2 equiv) in DMF (1 mL) over 10 min.

*Cleavage, Purification and Characterization of **21**−**27**.* The resulting resin-bound nucleopeptides **21**−**27** were washed exhaustively with DMF (5 × 1 min), DCM (5 × 1 min), and Et_2O (2 × 1 min) and then dried. Finally, **21**−**27** were cleaved from the resin by treatment with TFA/TIS/H_2O (95:2.5:2.5, 32 mL) for 3 h at rt (in the dark for **26** and **27**). The resin was filtered and the crude nucleopeptides precipitated from the TFA solution diluting to 15 mL with cold ethylic ether and then centrifuged (6000 rpm × 15 min). The supernatant was

DOI: 10.1021/acs.joc.6b01829
J. Org. Chem. 2016, 81, 11612−11625

carefully removed and the precipitate washed again with another aliquot of ethylic ether as described above. The so obtained wet solid was dried overnight under reduced pressure, redissolved in water/acetonitrile (9:1) and purified by reverse-phase HPLC (solvent A: water +0.1% TFA; solvent B: acetonitrile +0.1% TFA; from 0 to 90% of solvent B over 25 min, flow rate: 10 mL min^{-1}). Fractions of interest were evaporated under reduced pressure to remove the organic solvent and then lyophilized (in the dark for **26** and **27**). Obtained products were characterized by analytical HPLC and MALDI-TOF spectrometry. Yield, purity, retention times, and analytical data are reported as follows.

*Nucleopeptide **21***. 53.7 mg, overall yield: 80%, purity: ≥ 90%, ^{t}R 11.89 min (analytical HPLC, 10 to 90% acetonitrile in water (0.1% TFA) over 20 min, flow rate of 1.0 mL/min), MALDI-TOF Mass Spectrometry: Calculated: 2763.04 for $C_{116}H_{186}N_{49}O_{31}$ [M+H$^+$], found: 2762.45

*Nucleopeptide **22***. 50.4 mg, overall yield: 81%, purity: ≥ 90%, ^{t}R 11.35 min (analytical HPLC, 10 to 90% acetonitrile in water (0.1% TFA) over 20 min, flow rate of 1.0 mL/min), MALDI-TOF Mass Spectrometry: Calculated: 2593.94 for $C_{116}H_{185}N_{37}O_{31}$ [M+H$^+$], found: 2594.17

*Nucleopeptide **23***. 46.7 mg, overall yield: 96%, purity: ≥ 90%, ^{t}R 11.07 min (analytical HPLC, 10 to 90% acetonitrile in water (0.1% TFA) over 20 min, flow rate of 1.0 mL/min), MALDI-TOF Mass Spectrometry: Calculated: 2017.44 for $C_{86}H_{161}N_{37}O_{19}$ [M+H$^+$], found: 2018.26

*Nucleopeptide **26***. 57.96 mg, overall yield: 75%, purity: ≥ 95% after purification, ^{t}R 14.08 min (analytical HPLC, 10 to 90% acetonitrile in water (0.1% TFA) over 20 min, flow rate of 1.0 mL/min), MALDI-TOF Mass Spectrometry: Calculated: 3222.52 for $C_{141}H_{205}N_{51}O_{36}S$ [M+H$^+$], found: 3222.77

*Nucleopeptide **27***. 45.42 mg, overall yield: 62%, purity: ≥ 95% after purification, ^{t}R 14.05 min (analytical HPLC, 10 to 90% acetonitrile in water (0.1% TFA) over 20 min, flow rate of 1.0 mL/min), MALDI-TOF Mass Spectrometry: Calculated: 3052.29 for $C_{135}H_{181}N_{39}O_{42}S$ [M+H$^+$], found: 3053.89

*Synthesis of Nucleopeptide **28***. A Rink Amide AM-PS resin (50 mg, 0.48 mmol/g) was swelled, deprotected, and functionalized with Fmoc-L-Arg(Pbf)−OH by amide coupling reaction according to the procedure described for compounds **21**−**26**. Fmoc deprotection of the arginine residue was carried out by treatment with 20% (v/v) piperidine solution in DMF (1 × 5 min; 1 × 25 min) and then a positive Kaiser ninhydrine and TNBS tests were observed. Subsequenlty, the coupling of **2** was performed using 4 equiv (relative to the initial loading of the resin) of the amino acid. To a prestirred solution of the amino acid (53.1 mg, 4 equiv) with HBTU (36.4 mg, 4 equiv) and HOBt*H_2O (14.7 mg, 4 equiv) in DMF (1.5 mL), DIPEA (33.4 μL, 8 equiv) was added and the solution was poured to the preswollen resin. The mixture was shaken for 2 h at rt and then washed with DMF (3 × 1 min) and DCM (3 × 1 min). Fmoc was removed from Lys ε amino group by treatment with 20% (v/v) piperidine solution in DMF (1 × 5 min; 1 × 25 min) and then coupling with the nucleobase derivative was carried out using 4 equiv of the reactant. To a prestirred solution of **10** (38.1 mg, 4 equiv) with HBTU (36.4 mg, 4 equiv) and HOBt*H_2O (14.7 mg, 4 equiv) in DMF (1.5 mL), DIPEA (33.4 μL, 8 equiv) was added and the solution poured to the preswollen resin. The mixture was shaken for 2 h at rt and then washed with DMF (3 × 1 min) and DCM (3 × 1 min). Coupling completion was ascertained by negative Kaiser ninhydrine and TNBS tests and the remaining free amines were capped treating the resin with a solution of Ac_2O (4.5 μL, 2 equiv) and DIPEA (8.4 μL, 2 equiv) in DMF (1 mL) over 10 min. The *o*NBS protecting group was removed treating the resin with 500 μL of a centrifuged 5% (v/v) solution of thiophenol in dry DMF, previously saturated with 2 equiv (in respect to thiophenol) of K_2CO_3 (3 × 10 min). The resulting resin-bound nucleobase functionalized dipeptide was coupled with the following Fmoc-L-Arg(Pbf)−OH using 4 equiv of the amino acid, HBTU, HOBt, and 8 equiv of DIPEA and then elongated repeating the same synthetic steps as reported above. After the final *o*NBS removal, the *N*-terminal was acetylated adding a mixture of Ac_2O (4.5 μL, 2 equiv) and DIPEA (8.4 μL, 2 equiv) in DMF (1 mL) and shaking the resulting mixture over 30 min. The resin was washed exhaustively with DMF (5 × 1 min), DCM (5 × 1 min), and Et_2O (2 × 1 min) and then dried. Compound **28** was cleaved from the resin by treatment with TFA/TIS/H_2O (95:2.5:2.5, 2 mL) for 3 h at rt and the crude oligonucleopeptides were washed, purified, and collected following the same protocol as reported above. Yield, purity, retention times, and analytical data are reported as follows.

*Nucleopeptide **28***. 74.3 mg, overall yield: 83%, purity: ≥ 90%, ^{t}R 12.31 min (analytical HPLC, 10 to 90% acetonitrile in water (0.1% TFA) over 20 min, flow rate of 1.0 mL/min), MALDI-TOF Mass Spectrometry: Calculated: 3710.07 for $C_{153}H_{240}N_{81}O_{31}$ [M+H$^+$], found: 3711.14

UV and CD Procedures. UV measurements were acquired on a spectrophotometer equipped with a Peltier temperature programmer. Stock solutions of oligomers were prepared in doubly distilled and sterilized water and their concentration measured by UV at 260 nm at 90 °C using the following molar extinction coefficient: ε 260 (A) = 13.7 mL/(μmole × cm), ε 260 (C) = 6.6 mL/(μmole × cm), ε 260 (G) = 11.7 mL/(μmole × cm), ε 260 (T) = 8.8 mL/(μmole × cm). CD spectra and melting curves were acquired on a Circular Dichroism Spectrometer equipped with a Peltier temperature programmer. Both UV and CD spectra were acquired using 1 cm path-length quartz cells. Samples were lyophilized for 16 h. All hybridization experiments were carried out in a 10 mM phosphate buffer, 100 mM NaCl, pH 7.0. Duplexes were prepared by mixing equimolar concentrations of nucleopeptides with polydA (M.W. 330 Da; chain length 250−500 bases) (6 uM each base) and polyA (M.W. 100−500 Da; chain length 2100−10000 bases) (6 uM each base) and single stranded complementary DNA and RNA; annealing was performed incubating the samples at 90 °C for 5 min, then slowly cooling down at rt. Samples were kept at 4 °C overnight.[36] CD melting was monitored at 260 nm, with a scan rate of 1 °C min^{-1} in the 5−85 °C temperature range at λ = 247 nm and at λ = 267 nm for the duplexes with DNA, RNA oligomers, respectively. Melting temperatures were measured as the zero point of the second derivative of the melting curves. CD spectra were carried out in the 210−320 nm spectral window, keeping the temperature constant at 10 °C. For Job Plot linear fitting method was applied (R^2 = 0.9836).

Mass Spectrometry Procedures. Mass spectrometry analyses were performed with a matrix assisted laser desorption ionization time-of-flight (MALDI-TOF) mass spectrometer equipped with a pulsed nitrogen laser (λ = 337 nm). Prior to the acquisition of spectra, 1 μL of sample solution (100 pmol/μL) was mixed with 1 μL of saturated α-cyano-4- 4-hydroxycinnamic acid matrix solution (10 mg/mL in acetonitrile/trifluoroacetic acid 0.1%, 1:1, v:v) and a droplet of the resulting mixture (1 μL) placed on the mass spectrometer's sample target. The droplet was dried at rt. Once the liquid was completely evaporated, the sample was loaded into the mass spectrometer and analyzed in positive linear (molecular masses above 3000 Da) or reflectron mode. The instrument was externally calibrated in linear mode using a three points external calibration by using a mix of 10 pmol/μL of insulin, cytochrome-c, and trypsinogen as standards or using a 50 fmol/μL tryptic alcohol dehydrogenase digest in reflectron positive ion mode. The instrument source voltage was set at 12 kV. The accurate molecular mass of the 4/RNA duplex was determined on a ESI Q-TOF Micro mass spectrometer.

HPLC Procedures. The sample was RP-HPLC purified and solubilized in water at a concentration of 100 pmol/μL. Following a 1:10 dilution, the sample was infused into the system at a flow rate of 5 μL/min. The HPLC analyses were performed on a chromatograph equipped with a DAD detector. The crude oligomers were purified by HPLC using a preparative C18 reverse-phase column (150 × 21.2 mm, 100 Å, particle size 5 μm; solvent A: water +0.1% TFA; solvent B: acetonitrile +0.1% TFA; flow rate: 10 mL min^{-1}). Purified oligomers were characterized by UFLC equipped with an analytical C18 reverse-phase column (150 × 4.6 mm, 100 Å, particle size 5 μm; solvent A: water +0.1% TFA; solvent B: acetonitrile +0.1% TFA; flow rate: 1 mL min^{-1}).

Serum Biostability Assay Procedures. Serum stability was evaluated modifying a previously described protocol:[37] the reaction solution

DOI: 10.1021/acs.joc.6b01829
J. Org. Chem. 2016, 81, 11612−11625

was prepared by mixing nucleopeptide in sterile water (1 mM) and human serum (at concentration 0.1 mM, 90% serum) and incubated at 37 °C. Aliquots were taken at different times (30 min, 60 min, 120 min, 240 min), subjected to precipitation by addition of ACN/0.1% TFA solution, and then centrifuged (12 000 rpm, 15 min, 4 °C). The supernatant obtained was analyzed by HPLC using a linear elution gradient from 0% to 90% ACN (0.1% TFA) in water (0.1% TFA) in 30 min.

Cellular Uptake Procedures. Glioma cells were cultured in DMEM medium supplemented with 10% heat-inactivated FBS. All cells were cultured in a humidified incubator, containing 5% CO_2 at 37 °C. LN-299 cells growing in 24-well plates at the density of 10 × 103 cells/well for 24 h and were treated with FITC-labeled nucleopeptide (50 μM) for 1 and 3 h and then fixed using PBS 4% paraformaldehyde for 10 min and permeabilized for 10 min with PBS 0.1% Triton X-100. Cells were stained for 2 min at rt by 4′,6-diamidino-2-phenylindole, dihydrochloride (DAPI, 5 μ/mL), a nuclear and chromosome counterstain that emits blue fluorescence upon binding to AT regions of DNA. The cells were analyzed by confocal a microscope.

■ ASSOCIATED CONTENT

Supporting Information

The Supporting Information is available free of charge on the ACS Publications website at DOI: 10.1021/acs.joc.6b01829.

CD and UV Tm of hybrid duplexes; ^{1}H and ^{13}C spectra for compound **2**; HPLC profiles of **7**, **10**, and **14**; HPLC profiles and MALDI-TOF spectra of all the nucleopeptides (PDF)

■ AUTHOR INFORMATION

Corresponding Authors

*salvatore.dimaro@unina2.it

*anna.messere@unina2.it, anna.messere@gmail.com

Author Contributions

⊥M.E.M. and S.T. contributed equally

Notes

The authors declare no competing financial interest.

■ ACKNOWLEDGMENTS

This research was funded by Regione Campania under POR Campania FESR 2007-2013-O.O.2.1 (FarmaBioNet) to A.M. and S.C., Progetti di Rilevante Interesse Nazionale (PRIN) 2012 (2012CTAYSY_002) to S.C., Scientific Independence of Young Researchers (SIR) 2014 (RBSI142AMA) to S.D.M., and Legge Regionale 5/02 2008 [03-A00001366] to A.M.

■ REFERENCES

(1) Krützfeldt, J.; Rajewsky, N.; Braich, R.; Rajeev, K. G.; Tuschl, T.; Manoharan, M.; Stoffel, M. *Nature* **2005**, *438*, 685−689.

(2) Arenz, C. *Angew. Chem., Int. Ed.* **2006**, *45*, 5048−5050.

(3) Hayes, J.; Peruzzi, P. P.; Lawler, S. *Trends Mol. Med.* **2014**, *20*, 460−469.

(4) Wilson, C.; Keefe, A. D. *Curr. Opin. Chem. Biol.* **2006**, *10*, 607−614.

(5) Lennox, K. A.; Behlke, M. A. *Gene Ther.* **2011**, *18*, 1111−1120.

(6) Lau, N. C. *Science* **2001**, *294*, 858−862.

(7) Deleavey, G. F.; Damha, M. J. *Chem. Biol.* **2012**, *19*, 937−954.

(8) van Rooij, E.; Kauppinen, S. *EMBO Mol. Med.* **2014**, *6*, 851−864.

(9) Egholm, M.; Buchardt, O.; Nielsen, P. E.; Berg, R. H. *J. Am. Chem. Soc.* **1992**, *114*, 1895−1897.

(10) Fabani, M. M.; Gait, M. J. *RNA* **2007**, *14*, 336−346.

(11) Gaglione, M.; Milano, G.; Chambery, A.; Moggio, L.; Romanelli, A.; Messere, A. *Mol. BioSyst.* **2011**, *7*, 2490−2429.

(12) Koppelhus, U.; Awasthi, S. K.; Zachar, V.; Holst, H. U.; Ebbesen, P.; Nielsen, P. E. *Antisense Nucleic Acid Drug Dev.* **2002**, *12*, 51−63.

(13) Abes, S.; Turner, J. J.; Ivanova, G. D.; Owen, D.; Williams, D.; Arzumanov, A.; Clair, P.; Gait, M. J.; Lebleu, B. *Nucleic Acids Res.* **2007**, *35*, 4495−4502.

(14) Ljungstrøm, T.; Knudsen, H.; Nielsen, P. E. *Bioconjugate Chem.* **1999**, *10*, 965−972.

(15) Milano, G.; Musumeci, D.; Gaglione, M.; Messere, A. *Mol. BioSyst.* **2010**, *6*, 553−561.

(16) Sahu, B.; Chenna, V.; Lathrop, K. L.; Thomas, S. M.; Zon, G.; Livak, K. J.; Ly, D. H. *J. Org. Chem.* **2009**, *74*, 1509−1516.

(17) Moggio, L.; Romanelli, A.; Gambari, R.; Bianchi, N.; Borgatti, M.; Fabbri, E.; Mancini, I.; di Blasio, B.; Pedone, C.; Messere, A. *Biopolymers* **2007**, *88*, 815−822.

(18) Dragulescu-Andrasi, A.; Zhou, P.; He, G.; Ly, D. H. *Chem. Commun.* **2005**, 244−246.

(19) Geotti-Bianchini, P.; Beyrath, J.; Chaloin, O.; Formaggio, F.; Bianco, A. *Org. Biomol. Chem.* **2008**, *6*, 3661−3663.

(20) Roviello, G. N.; Ricci, A.; Bucci, E. M.; Pedone, C. *Mol. BioSyst.* **2011**, *7*, 1773−1778.

(21) Fujii, M.; Yoshida, K.; Hidaka, J.; Fujii, M.; Yoshida, K.; Hidaka, J.; Ohtsu, T. *Chem. Commun.* **1998**, 717−718.

(22) Schwarze, S. R.; Ho, A.; Vocero-Akbani, A.; Dowdy, S. F. *Science* **1999**, *285*, 1569.

(23) Roviello, G. N.; Vicidomini, C.; Di Gaetano, S. D.; Capasso, D.; Musumeci, D.; Roviello, V. *RSC Adv.* **2016**, *6*, 14140−14148.

(24) Diederichsen, U. *Angew. Chem., Int. Ed. Engl.* **1996**, *35*, 445−448.

(25) Fukuyama, T.; Jow, C.-K.; Cheung, M. *Tetrahedron Lett.* **1995**, *36*, 6373−6374.

(26) Mas-Moruno, C.; Beck, J. G.; Doedens, L.; Frank, A. O.; Marinelli, L.; Cosconati, S.; Novellino, E.; Kessler, H. *Angew. Chem., Int. Ed.* **2011**, *50*, 9496−9500.

(27) Miller, S. C.; Scanlan, T. S. *J. Am. Chem. Soc.* **1998**, *120*, 2690−2691.

(28) Varghese, J.; (Elan Pharmaceuticals, Inc., Pharmacia & Upjohn Company, USA); Preparation of amino acid derivatives useful for the treatment of Alzheimer's disease, WO 2003045378, January 5 2003.

(29) Porcheddu, A.; Giacomelli, G.; Piredda, I.; Carta, M.; Nieddu, G. *J. Org. Chem.* **2008**, *34*, 5786−5797.

(30) Kaneko, T.; Aso, M.; Koga, N.; Suemune, H. *Org. Lett.* **2005**, *7*, 303−306.

(31) Baraldi, P. G.; Preti, D.; Zaid, A. N.; Saponaro, G.; Tabrizi, M. A.; Baraldi, S.; Romagnoli, R.; Moorman, A. R.; Varani, K.; Cosconati, S.; Di Maro, S.; Marinelli, L.; Novellino, E.; Borea, P. A. *J. Med. Chem.* **2011**, *54*, 5205−5220.

(32) Fukuyama, T.; Cheung, M.; Kan, T. *Synlett* **1999**, *1999*, 1301−1303.

(33) Kaiser, E.; Colescott, R.; Bossinger, C.; Cook, P. *Anal. Biochem.* **1970**, *34*, 595−598.

(34) Hancock, W.; Battersby, J. *Anal. Biochem.* **1976**, *71*, 260−264.

(35) Wada, T.; Minamimoto, N.; Inaki, Y.; Inoue, Y. *J. Am. Chem. Soc.* **2000**, *122*, 6900−6910.

(36) Gaglione, M.; Potenza, N.; Di Fabio, G.; Romanucci, V.; Mosca, N.; Russo, A.; Novellino, E.; Cosconati, S.; Messere, A. *ACS Med. Chem. Lett.* **2013**, *4*, 75−78.

(37) Di Maro, S.; Trotta, A. M.; Brancaccio, D.; Di Leva, F. S.; La Pietra, V.; Ieranò, C.; Napolitano, M.; Portella, L.; D'Alterio, C.; Siciliano, R. A.; Sementa, D.; Tomassi, S.; Carotenuto, A.; Novellino, E.; Scala, S.; Marinelli, L. *J. Med. Chem.* **2016**, *59*, 8369−8380.

DOI: 10.1021/acs.joc.6b01829
J. Org. Chem. 2016, 81, 11612−11625